OAHU HAWAIIAN HOARY BAT
OCCUPANCY AND DISTRIBUTION STUDY

Project Update and Second Year Analysis

Prepared for:

Hawaii Endangered Species Research Committee

Prepared by:

**Leigh Ann Starcevich, Joel Thompson, Troy Rintz,
Erica Adamczyk, Mysti Martin, and Donald Solick**

Western EcoSystems Technology, Inc.
2725 NW Walnut Boulevard
Corvallis, Oregon 97330

February 13, 2020

Privileged and Confidential - Not For Distribution

TABLE OF CONTENTS

LIST OF TABLES

LIST OF FIGURES

LIST OF APPENDICES

INTRODUCTION

In response to a request for proposals issued in 2016 by Hawaii's Endangered Species Recovery Committee (ESRC), Western EcoSystems Technology, Inc. (WEST) developed a 5-year study proposal to investigate the distribution and seasonal occupancy of Hawaiian hoary bat (HAHOBA; *Lasiurus cinereus semotus*) on the island of Oahu. The initial study proposal, submitted in fall 2016, was modified as a result of two meetings and discussions with the ESRC Bat subcommittee, which occurred in January and February, 2017. Based on discussions with the ESRC and Bat subcommittee, it was decided the initial goals of the study should be to examine the distribution and seasonal occupancy of HAHOBA, with study plans for subsequent years to be based on the results of the initial year(s) of data.

A final study plan developed in early 2017 that focused on HAHOBA distribution and occupancy was considered to be consistent with the recommendations and priorities of the ESRC bat subcommittee. The objectives of the study were to 1) provide information on bat occupancy, distribution, and detection probabilities for the island of Oahu, 2) examine seasonal changes in distribution by estimating seasonal changes in occupancy, and 3) collect data that could be used later to assess HAHOBA habitat use relationships.

While field studies are ongoing, the second year of data collection for the HAHOBA Occupancy and Distribution Study (Occupancy Study) has been completed. This preliminary report has been developed to update the ESRC and other cooperating entities on the status of the Occupancy Study and initial analysis results.

In this report, we describe the sampling design and methods used to collect and analyze the data. We then summarize the results of the second year of field studies and occupancy analysis, and conclude with recommendations for ongoing studies and future analysis. This report is an interim update based on the data available to date (as of October 2019); therefore, readers should recognize that this interim report addresses only the first approximately two years of data from a multi-year project and revised analyses that may affect interpretation of results will be forthcoming as the study progresses.

METHODS

In this section, we describe the sampling design, field data collection methods, and occupancy modeling techniques used to address HAHOBA distribution on Oahu.

Sampling Design

The sampling design was developed to form the basis for island-wide inference. A sampling frame of 787 grid cells was obtained by overlaying a grid of 0.8 square miles (2.3 square kilometers) cells across the island of Oahu. To allow for island-wide inference, no areas on Oahu were omitted from the sampling frame except for small nearshore islands. From the grid of 787 cells, an equiprobable generalized random tessellation stratified sample (Stevens and Olsen 2003, 2004) of 100 grid cells was selected for placement of acoustic bat detectors (Figure 1). An oversample of 150 grid cells was also selected to provide an extra set of spatially balanced sites to use if the main sample of 100 grid cells could not be completely surveyed. Reasons a grid cell might not be surveyed every year include inaccessibility due to safety issues, landowner denial of access, and possible relocation of detectors to new grid cells if the sampling design is amended.

Field Data Collection

Wildlife Acoustics Song Meter SM4Bat (SM4) full spectrum bat detectors fitted with model SMM-U1 ultrasonic microphones (Wildlife Acoustics, Inc., Concord, Massachusetts) were initially deployed for all data collection conducted by WEST; however, SMM-U1 microphones started to malfunction in April 2019 and Wildlife Acoustics recommended updating to SMM-U2 ultrasonic microphones (Wildlife Acoustics, Inc., Concord, Massachusetts). New SMM-U2 microphones were deployed throughout summer and fall 2019 when a maintenance check was required. Microphone type was recorded so that microphone effects could be examined as a covariate in detection probability models. Data from cooperating entities sometimes was collected using older Wildlife Acoustics full spectrum bat detectors (e.g., SM3Bat) outfitted with SMM-U1 microphones. The SM4 detectors are small, measuring roughly eight inches (in) tall x five in wide x three in deep (20 centimeters [cm] tall x 13 cm wide x eight cm deep) and are fully self-contained (Figure 2). Some of the detectors located in easily accessible areas with relatively high risk of theft or vandalism were operated on internal batteries to minimize their detectability by people, while most detectors utilized a small external battery and accompanying solar panel as a power source (Figure 2).

Detectors were attached to existing structures (e.g., fence posts, light poles) or newly installed t-posts, via attachment of a 10-foot (ft; 3-meter) length of 0.75 in (1.9 cm) diameter metal conduit used to extend the microphone to approximately three m above ground (Figure 2). In some cases, the 10-ft pole was supported by small guy wires. The detector, and external battery and solar panels (when used), were mounted low on the pole with the microphone mounted at the top of the pole (Figure 2). In some developed areas, units were contained in a small (about 15 in [38 cm]) toolbox and placed on top of an appropriately sized outbuilding (approximately 10 ft above ground).

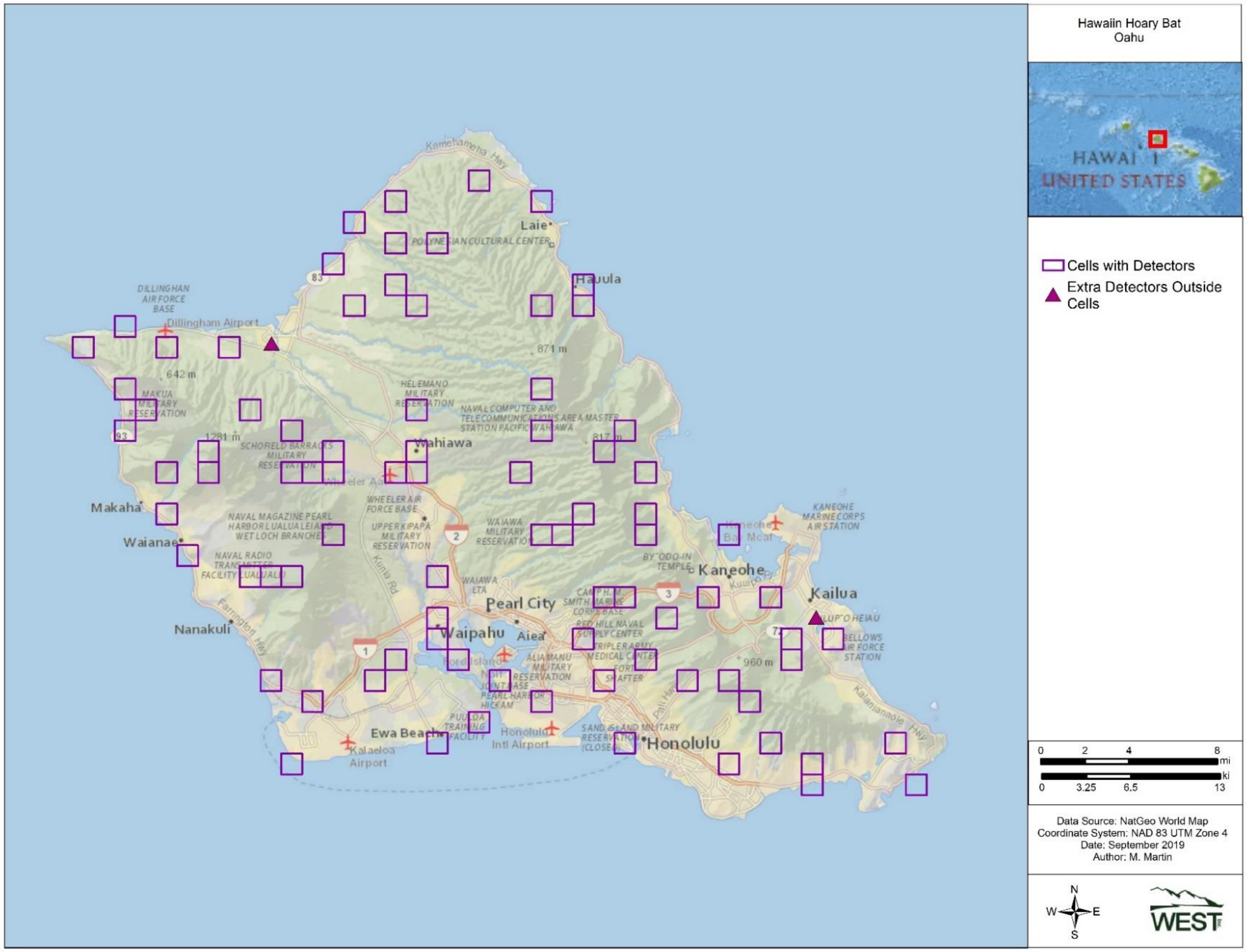

Figure 1: Equiprobable generalized random tessellation stratified sample of 100 grid cells used for initial study design of the island-wide occupancy study of Hawaiian hoary bats on Oahu.

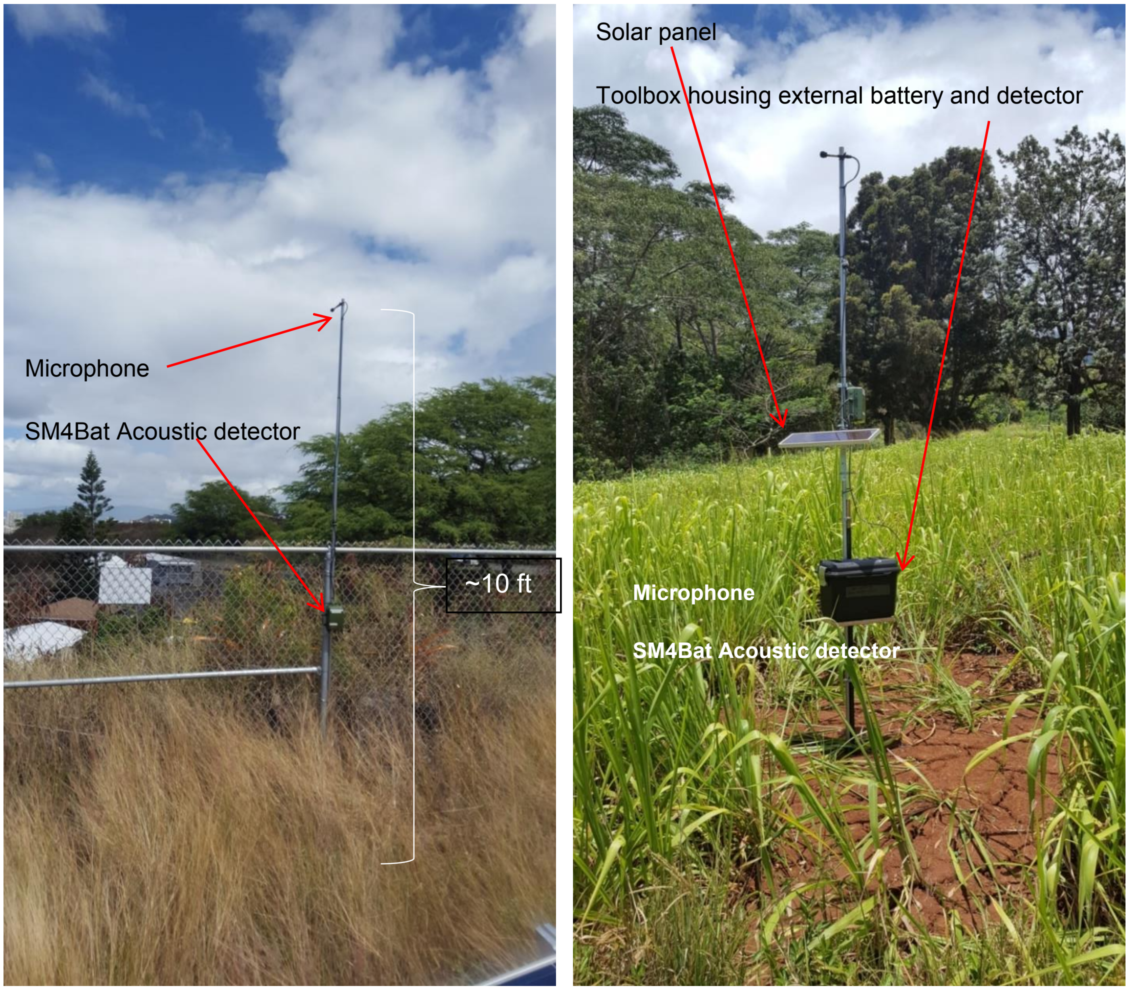

Figure 2. Examples of commonly used set-ups of the Wildlife Acoustics SM4Bat detectors used in the Hawaiian hoary bat Occupancy and Distribution study on Oahu.

Detectors remained in the field year round at the location of original placement. Detectors were programmed to operate nightly, from approximately one hour prior to sunset to approximately one hour after sunrise. Within the SM4 Detector Configurator, the following settings were selected: detector sample rate of 192 kilohertz (kHz); gain of 12 decibels (dB); minimum signal duration of 1.5 milliseconds; maximum signal duration off; minimum trigger frequency of 10 kHz; trigger level of 12 dB; and trigger window of three seconds. Detectors were visited regularly to swap data cards and ensure detectors were functioning properly. Following initial set-up, detectors were checked once seven to 14 days after deployment to ensure proper function and data collection. After these initial checks, sites were checked less frequently. At sites with external power sources, detectors were checked every one to two months, while sites that mandated helicopter access sometimes extended to more than two months between checks. At sites where the detectors were powered by internal batteries, units would be visited every 10−14 days on average.

To expedite call analysis, call recordings were processed with the Kaleidoscope Pro 5 software package (Wildlife Acoustics 2019) to convert the full-spectrum call files to zero-cross files and remove noise (i.e., non-bat) files. For all files classified as containing a bat echolocation call, a biologist manually reviewed the zero-cross call files using program Analook (Titley Scientific) to ensure detections contained a minimum of two distinct pulses and confirm the recording was consistent with that of a HAHOBA. Manual review of all recorded bat calls by a bat biologist helped minimize the potential for false positives to be included in the final dataset. Social calls and feeding buzzes were also noted during the manual review process for later assessment of behavioral activity at sites. Initially, some call files were recorded as having multiple individuals in a single file; however, upon further review and discussion with other acoustic call experts, it was decided these call files be reassigned to a single individual. A subset of noise files was also examined to ensure detectors were functioning properly when several consecutive nights with no recordings occurred.

Occupancy modeling

Nightly detector data were used to model occupancy rates and detection probabilities of HAHOBA on Oahu (MacKenzie et al. 2006), with the appropriate model type depending on model assumptions. Multi-season dynamic occupancy models that account for site-level extinction (the probability an occupied site will be unoccupied the next season) and local colonization (the probability an unoccupied site will be occupied the next season) were implemented to meet the closure assumption within a season. We used the HAHOBA reproductive season definitions of Gorresen et al. (2013, as adapted from Menard 2001) as the basis for our seasonal models: lactation season from mid-June to August, post-lactation season from September to mid-December, pre-pregnancy season from mid-December to March, and pregnancy season from April to mid-June. Differences in detections among seasons could be due to a seasonal detection effect, differences in occupancy by season, or both. We examined two dynamic occupancy models: the multi-season dynamic occupancy model where detections are assumed independent (MacKenzie et al. 2006), and the multi-season dynamic occupancy model that assumes detections are correlated (Hines et al. 2010, 2014). Independent occupancy modeling was conducted with the *unmarked* package (Fiske and Chandler 2011) in R (R Development Core Team 2016).

The multi-season dynamic occupancy model for independent detections (MacKenzie et al. 2006) yields estimates of rates of occupancy (Ψ), detection (p), local extinction (ε), and local colonization (γ). This model requires assumptions of equal probability of occupancy across sites, equal probability of detection across sites, population closure within each season, independence of detections across sites, and independence among detections at a site. The first two assumptions can be relaxed if covariates related to the occupancy and detection processes are included in the models. We assume independence among sites based on the probabilistic and spatially balanced sampling design. Independence among detections at a site may be violated if detections observed over time are temporally correlated. When temporal correlation is present, detection occasions may be separated in time to avoid temporal correlation (Wright et al. 2016). We evaluated the independence of nightly detection data within each reproductive season and year with the join count chi-square test (Wright et al. 2016). The join count test compares the number of temporal "joins" (number of detections in consecutive time periods) to an expected number based on the assumption of independence. We applied the join count test to data sets obtained from systematic random samples of detector nights taken by site at various intervals to determine the appropriate temporal spacing of detector nights to meet the assumption of independent sampling occasions for a given site. We also used the join count test to examine the assumption of a first-order Markov detection process (Hines et al. 2010, 2014) to account for correlated detections. For this model, estimates of occupancy (Ψ), local extinction (ε), and local colonization (γ) are obtained, but the probability of detection (p) is conditional on local presence for the current and previous sampling occasion. The Markov model computes the probability of local presence conditional on presence or absence of HAHOBA during the previous survey occasion, and estimates of the detection probability differ based on the detection of HAHOBA during the previous detection night. Correlated detection occupancy modeling was conducted in program PRESENCE (US Geological Survey [USGS] 2019). Site-level covariates representing elevation, the percentage of trees, and human population density in each grid cell were also examined as predictors in occupancy models.

RESULTS

Data collection began in June 2017 and has been ongoing since. Gaining access to sample sites progressed steadily, but more slowly than anticipated in the original proposal. Ultimately, while our initial goal was to deploy 100 detectors across Oahu, we were unable to do achieve the goal of 100 detectors in Year 1 using the probabilistic sampling design. Land access was the most common reason for not getting units deployed within sequentially selected cells, with lack of suitable sample sites also causing some cells to be skipped. Land access issues were most often associated with cells mostly owned and or managed by larger private landowners (e.g., agricultural entities and developers) that would not grant permission or from whom we could not get a response to our request for access. Lack of suitable sites within cells resulted from a lack of safely accessible sites or simply the lack of a suitable location to mount or locate a detector. As a result, we extended our sample effort to include 19 of the oversample cells; however, these same issues also affected some of the oversample cells.

In total, WEST placed 86 detectors in the field during the study period, with 84 of the 86 located in the randomly selected grid cells and two located at sites not within randomly selected cells (Figure 3). One additional randomly selected grid cell is located in the Kuhuku Wind Project. Data from one detector randomly selected from the two already being monitored in the Kuhuku Wind Project grid cell has been provided by TerraForm Power. This brings the maximum number of detectors being monitored at any one time to 87. Due to vandalism and repeated theft, detectors at two locations (Malekahana State Park and Ewa Beach Park) are no longer in service, having been eliminated from the sample after the last theft at each location. Of the two detectors not placed in randomly selected cells, one was initially used as a test site and is located in Waialua at the home of WEST's field biologist, while the other was placed at Hamakua Ponds at the request of the Department of Forestry and Wildlife staff. WEST has collected, processed, and incorporated data from the 85 detectors placed in randomly selected grid cells into the current analysis.

Detectors were placed in the field as access permissions were obtained, therefore, the temporal distribution of data varied among detectors. As such, seasonal data sets differ in the number of detectors that contributed data.

Detector Data

Total Detections

Data available as of October 2019 were processed and include detections collected between June 8, 2017, and October 7, 2019. Some of the detectors operating through October 7, 2019, were not yet processed at the time of data analysis and will be included in future analyses. At least one bat detection was recorded at 77 of the 87 (89%) sites over the full time period (June 2017 through October 2019). The number of detector nights sampled by site ranged from 106 to 800 (Table 1) for the full time period, and 12,185 HAHOBA detections were recorded; 4,978 detections in Year 1 and 5,315 detections in Year 2. Site-level detections ranged from zero to 2,551 for the full time period (median = 11 detections), with a range of zero to 1,524 for Year 1 (median = two detections; Figure 4a) and zero to 1,592 for Year 2 (median = five detections; Figure 4b).

Detections per Detector Night

The mean number of site-level detections per detector night ranged from zero to 4.18 overall (Table 1), from zero to 4.37 in Year 1 (Figure 5a), and from zero to 5.19 in Year 2 (Figure 5b). Detections were more widespread across Oahu during the post-lactation season relative to the other seasons in both Year 1 (Figure 6a) and Year 2 (Figure 6b).

Proportion of Detector Nights

The proportion of detector nights with detections ranged from zero to 0.40 (Table 1) across all seasons and sites for the full time period, from zero to 0.52 for Year 1 (Figure 7a), and from zero to 0.37 for Year 2 (Figure 7b). The proportion of detector nights with detections for Year 1 (Figure 8a) and Year 2 (Figure 8b) demonstrated similar seasonal patterns to those of mean detections per detector night.

Feeding Buzzes and Social Calls

For the full time period (June 2017 through October 2019), feeding buzzes (1,391 detections) and social calls (101 detections) were identified from call files recorded at 39 detectors (Figure 9). The presence of feeding buzzes and social calls is reported here for informational purposes, but may be incorporated into future analyses in a more formal way.

Table 1. Total detections, total detector nights, mean detections per night, and proportion of nights with detections by site from June 2017 – October 2019.

Site ID	Site Name	Detections	Nights with Detections	Detector Nights‡	Mean Detections Per Detector Night	Proportion of Detector Nights with Detections
Site-000	Goodale Tribe*	37	34	745	0.0497	0.0456
Site-002	TTHTT	31	27	754	0.0411	0.0358
Site-004	Army Nat Res	20	19	767	0.0261	0.0248
Site-006	Waihee Res	0	0	420	0	0
Site-008	Ewa Beach Park[a]	0	0	106	0	0
Site-009	Waianae HS	14	13	666	0.0210	0.0195
Site-011	Burn Camp	40	32	713	0.0561	0.0449
Site-013	KAW Gate	357	157	698	0.5115	0.2249
Site-016	Radar Hill Rd	8	7	350	0.0229	0.0200
Site-018	Dillingham Air	30	28	673	0.0446	0.0416
Site-020	Wahiawa botanical	17	16	765	0.0222	0.0209
Site-021	Lualualei 1	183	76	660	0.2773	0.1152
Site-022	Kahana Wedding	8	5	673	0.0119	0.0074
Site-023	Waimea Valley	630	241	754	0.8355	0.3196
Site-024	Ft Shafter	3	3	747	0.0040	0.0040
Site-025	Schofield	127	94	767	0.1656	0.1226
Site-026	Kawainiui	0	0	693	0	0
Site-029	KAW Rd	84	70	598	0.1405	0.1171
Site-030	Sacred Falls	1	1	584	0.0017	0.0017
Site-031	Plantation Village	4	4	737	0.0054	0.0054
Site-032	Nuuanu Watershed	0	0	588	0	0
Site-033	Camp Erdman	36	28	745	0.0483	0.0376
Site-034	Barbers Point	2	2	604	0.0033	0.0033
Site-035	Helemano	42	39	717	0.0586	0.0544
Site-036	Kroc Center	3	3	650	0.0046	0.0046
Site-038	Moanalua Trail	1	1	706	0.0014	0.0014
Site-039	Pupukea	2391	215	767	3.1173	0.2803
Site-040	Hickham AFB	0	0	549	0	0
Site-041	Schofield 3	339	180	730	0.4644	0.2466
Site-043	Manana Trail 1	2	2	800	0.0025	0.0025
Site-044	Royal Hawaiian Golf	2	2	668	0.0030	0.0030
Site-046	Poamoho	11	10	721	0.0153	0.0139
Site-048	Chaminade Univ.	6	6	789	0.0076	0.0076
Site-049	Lualualei NAVY	23	19	590	0.0390	0.0322
Site-050	HECO Kahe Point	5	3	786	0.0064	0.0038
Site-053	Kumaipo LZ	2551	247	610	4.1820	0.4049
Site-054	Anchor Church	2	2	591	0.0034	0.0034
Site-055	Schofield Waikane	24	18	696	0.0345	0.0259
Site-057	McCarthy Field	147	109	767	0.1917	0.1421
Site-058	Kailua Heights	4	3	618	0.0065	0.0049

Table 1. Total detections, total detector nights, mean detections per night, and proportion of nights with detections by site from June 2017 – October 2019.

Site ID	Site Name	Detections	Nights with Detections	Detector Nights‡	Mean Detections Per Detector Night	Proportion of Detector Nights with Detections
Site-059	Moanalua Red Hill	2	2	574	0.0035	0.0035
Site-060	Hawaii Loa Booster	11	11	605	0.0182	0.0182
Site-061	Mt Kaala	294	206	767	0.3833	0.2686
Site-064	Kamehameha Res	16	14	456	0.0351	0.0307
Site-065	Makua Valley	18	14	620	0.0290	0.0226
Site-066	Wheeler	37	32	711	0.0520	0.0450
Site-067	Honouliuli FR	14	11	644	0.0217	0.0171
Site-068	Waikane Valley	1	1	552	0.0018	0.0018
Site-069	MitchDetector	6	4	721	0.0083	0.0055
Site-070	Iroquois Pt	6	5	519	0.0116	0.0096
Site-071	Makaha Res	12	8	524	0.0229	0.0153
Site-072	Waihee Wells	0	0	482	0	0
Site-073	Kipapa North Fence	0	0	271	0	0
Site-074	Hawaii Loa	37	20	605	0.0612	0.0331
Site-075	Peerson	2386	272	715	3.3371	0.3804
Site-076	Kaipapau FR	31	8	712	0.0435	0.0112
Site-077	Manana Trail 2	4	4	760	0.0053	0.0053
Site-078	Sand Island	1	1	728	0.0014	0.0014
Site-079	Makua Ridge	229	113	724	0.3163	0.1561
Site-081	KAW 2	66	60	710	0.0930	0.0845
Site-083	Lualualei 2	128	71	680	0.1882	0.1044
Site-084	Aiea Loop Ridge	4	4	664	0.0060	0.0060
Site-085	Kaw 1	51	48	774	0.0659	0.0620
Site-087	Schofield 1	86	67	718	0.1198	0.0933
Site-088	Kawainui Marsh 1	0	0	739	0	0
Site-089	Waiawa Snot	6	3	790	0.0076	0.0038
Site-090	Kau Crater Trail	1	1	656	0.0015	0.0015
Site-093	Pouhala Marsh	7	7	702	0.0100	0.0100
Site-094	Manoa Falls	6	5	787	0.0076	0.0064
Site-095	Kuaokala Game Area	30	21	632	0.0475	0.0332
Site-097	Malaekahana SP	152	14	509	0.2986	0.0275
Site-098	West Loch Golf	8	8	632	0.0127	0.0127
Site-100	Heeia State Park	5	4	694	0.0072	0.0058
Site-101	Pupukea Paumalu	348	163	413	0.8426	0.3947
Site-102	Pearl Harbor	4	4	586	0.0068	0.0068
Site-103	Schofield Forest	483	116	743	0.6501	0.1561
Site-105	Aiea Loop Trail 1	170	37	745	0.2282	0.0497
Site-106	Puu Pia Trail	2	2	556	0.0036	0.0036
Site-109	Central Oahu Park	9	9	550	0.0164	0.0164

Table 1. Total detections, total detector nights, mean detections per night, and proportion of nights with detections by site from June 2017 – October 2019.

Site ID	Site Name	Detections	Nights with Detections	Detector Nights‡	Mean Detections Per Detector Night	Proportion of Detector Nights with Detections
Site-110	Halone Blowhole	0	0	580	0	0
Site-111	YMCA Waianae	11	9	410	0.0268	0.0220
Site-112	Barbers Point	0	0	520	0	0
Site-113	Hauula Dist. Park	2	2	562	0.0036	0.0036
Site-114	Waipio Soccer	1	1	531	0.0019	0.0019
Site-115	Waianae Valley	274	63	714	0.3838	0.0882
Site-119	Makua Cave	37	32	550	0.0673	0.0582
Site-999	Hamakua Pond*	4	4	672	0.0060	0.0060

* Denotes subjectively selected grid cells.

‡ Denotes nights that the detector was functional.

[a] data from a single season only.

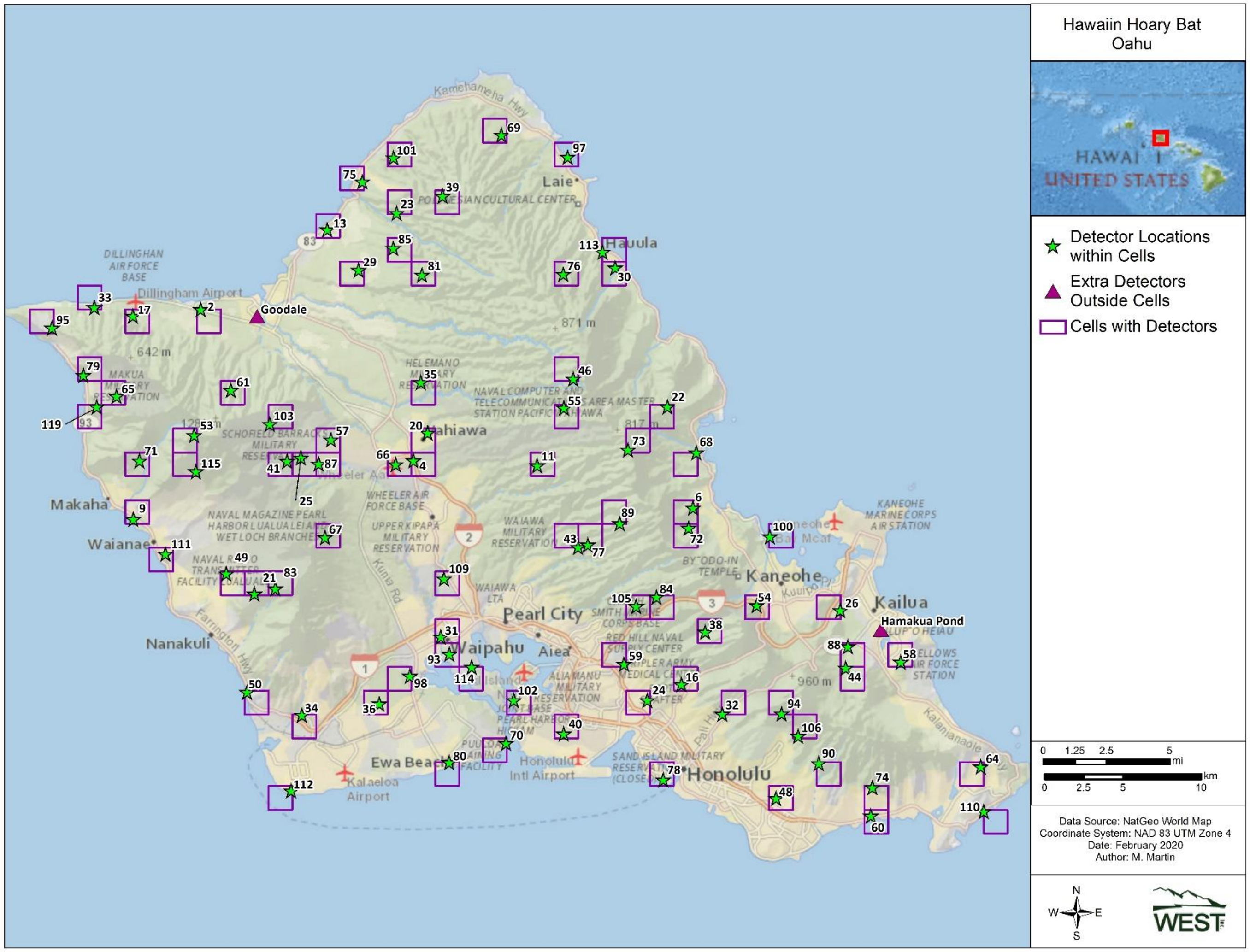

Figure 3: Distribution of acoustic bat detectors used in the island-wide occupancy study of Hawaiian hoary bats on Oahu. Site identification numbers are provided for each sample location.

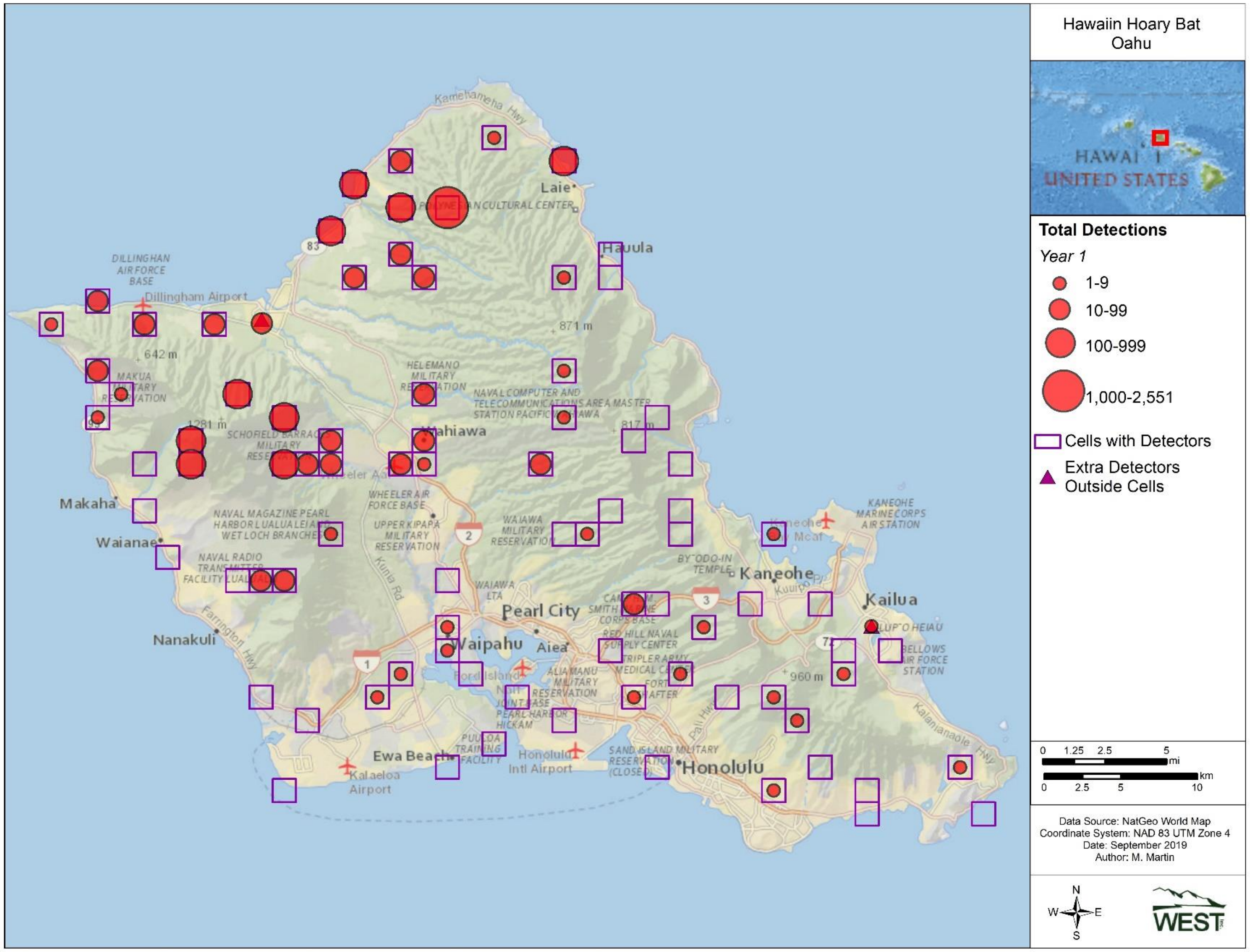

Figure 4a: Total detections by site between June 2017 and June 2018.

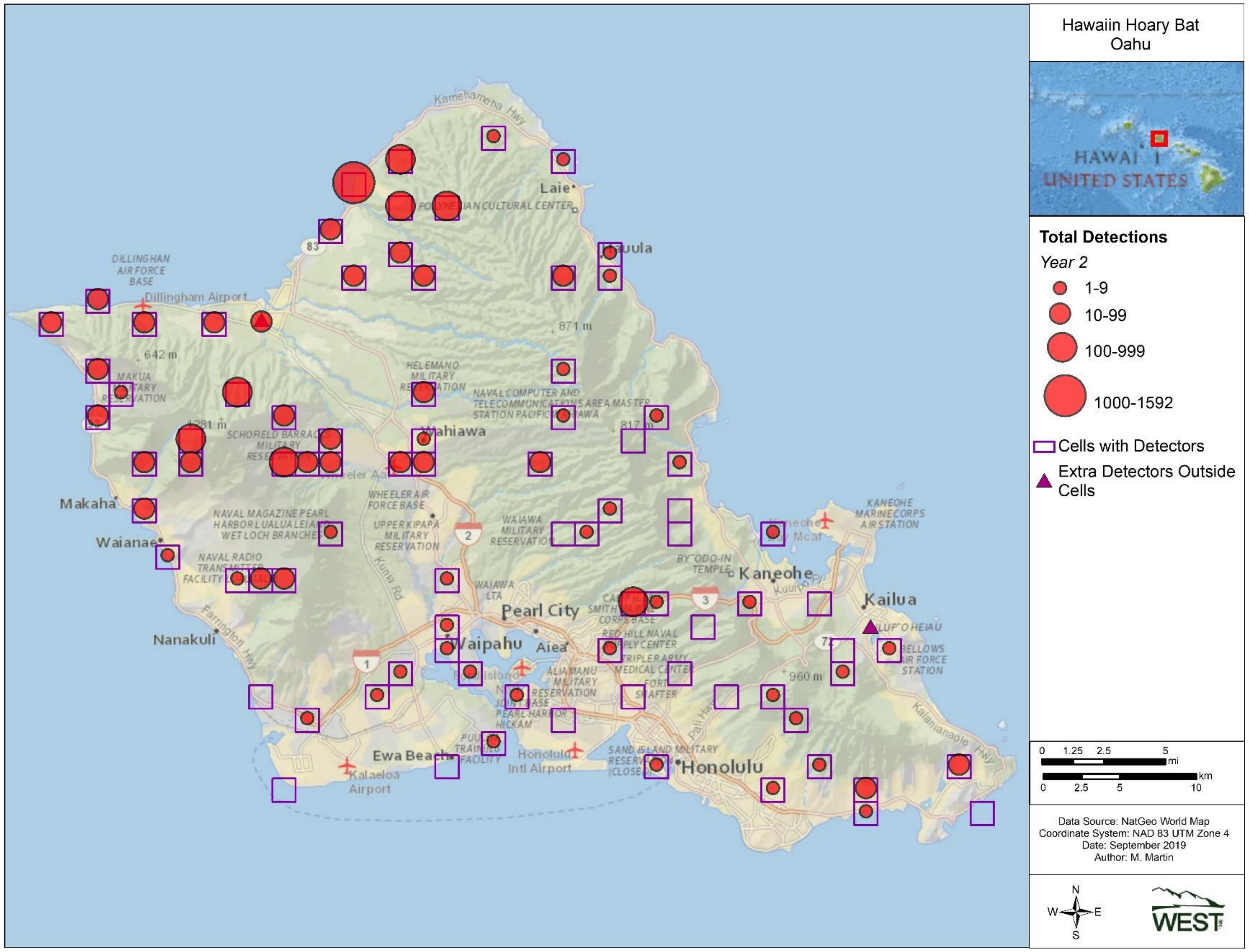

Figure 4b: Total detections by site between June 2018 and June 2019.

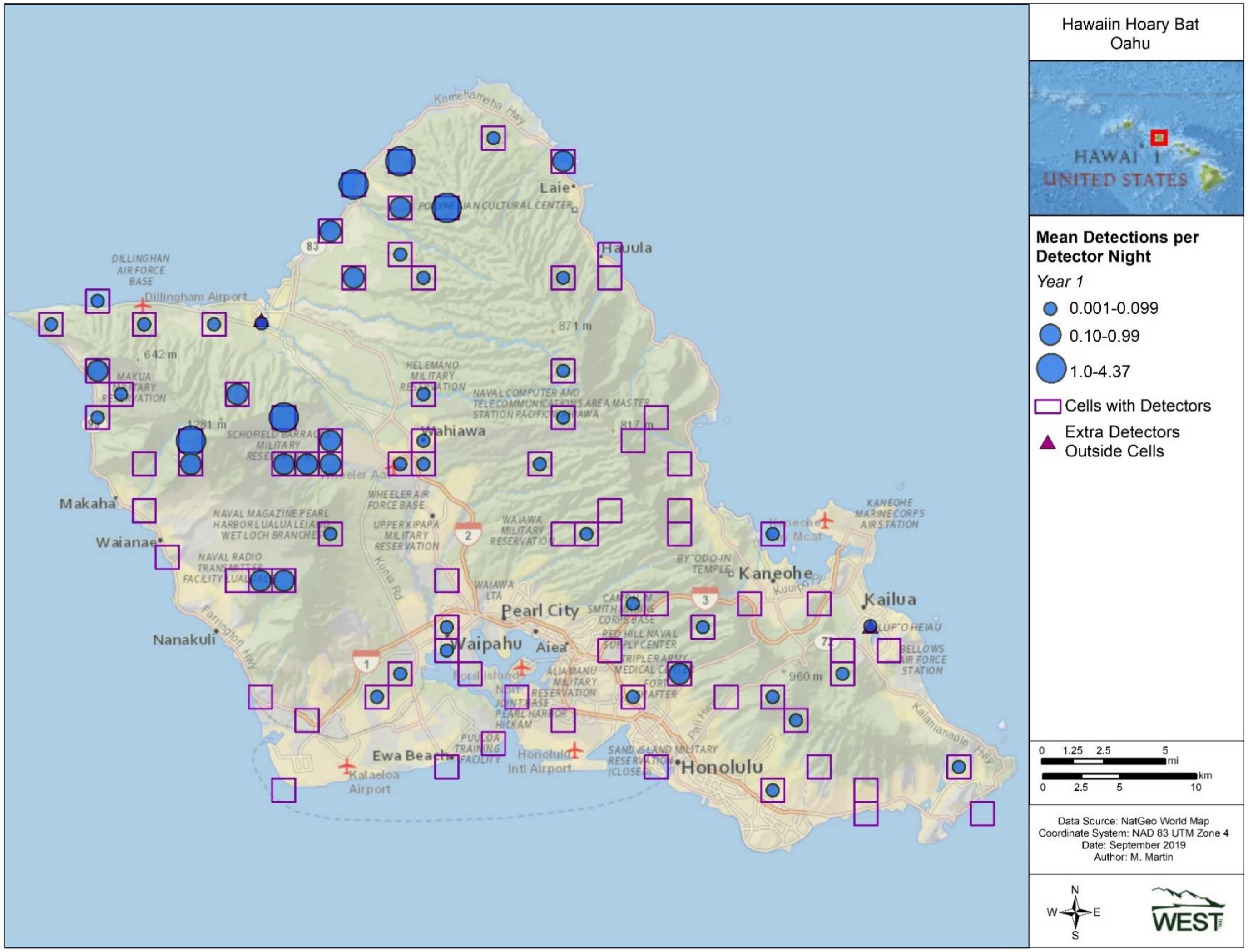

Figure 5a: Mean detections per night by site between June 2017 and June 2018.

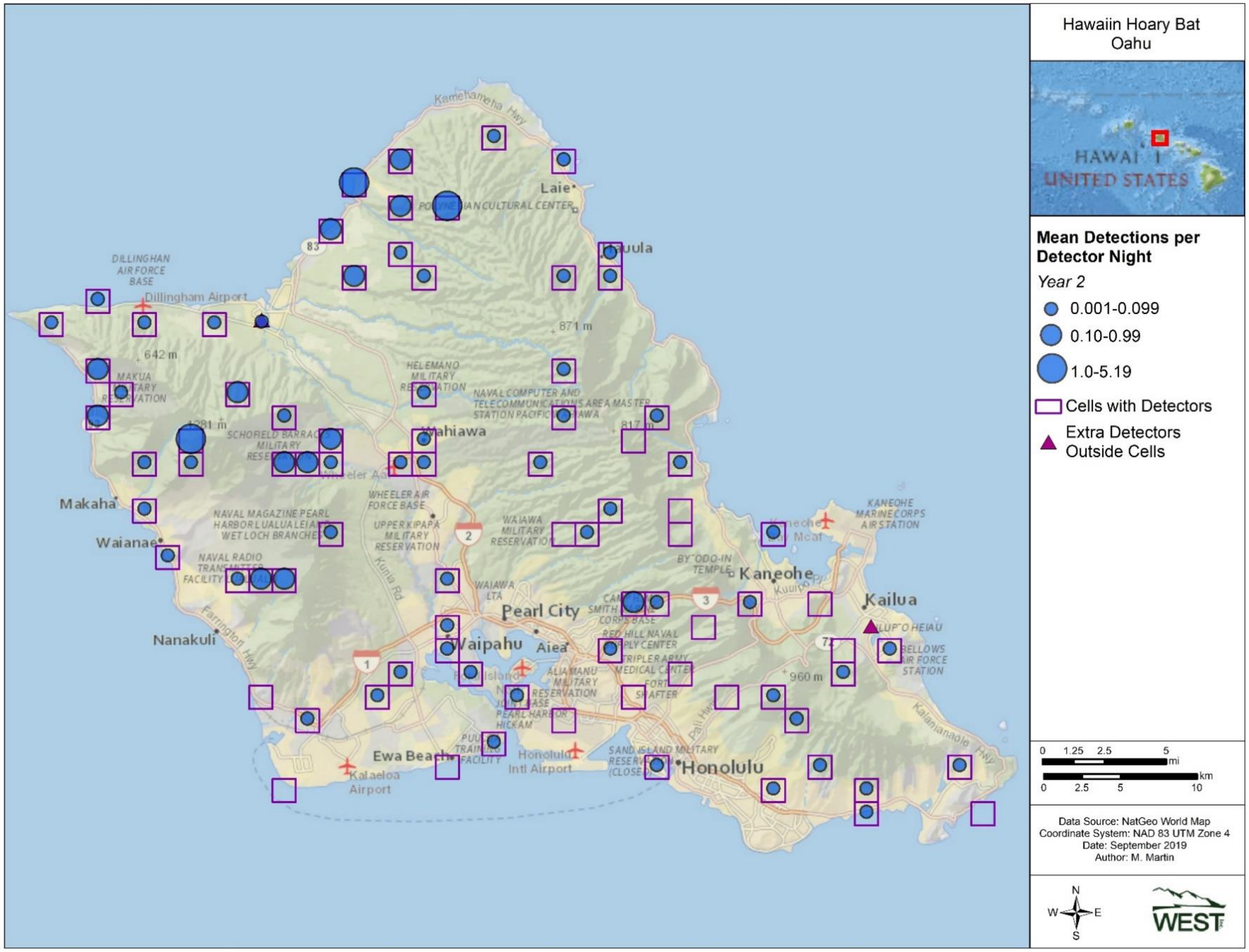

Figure 5b: Mean detections per night by site between June 2018 and June 2019.

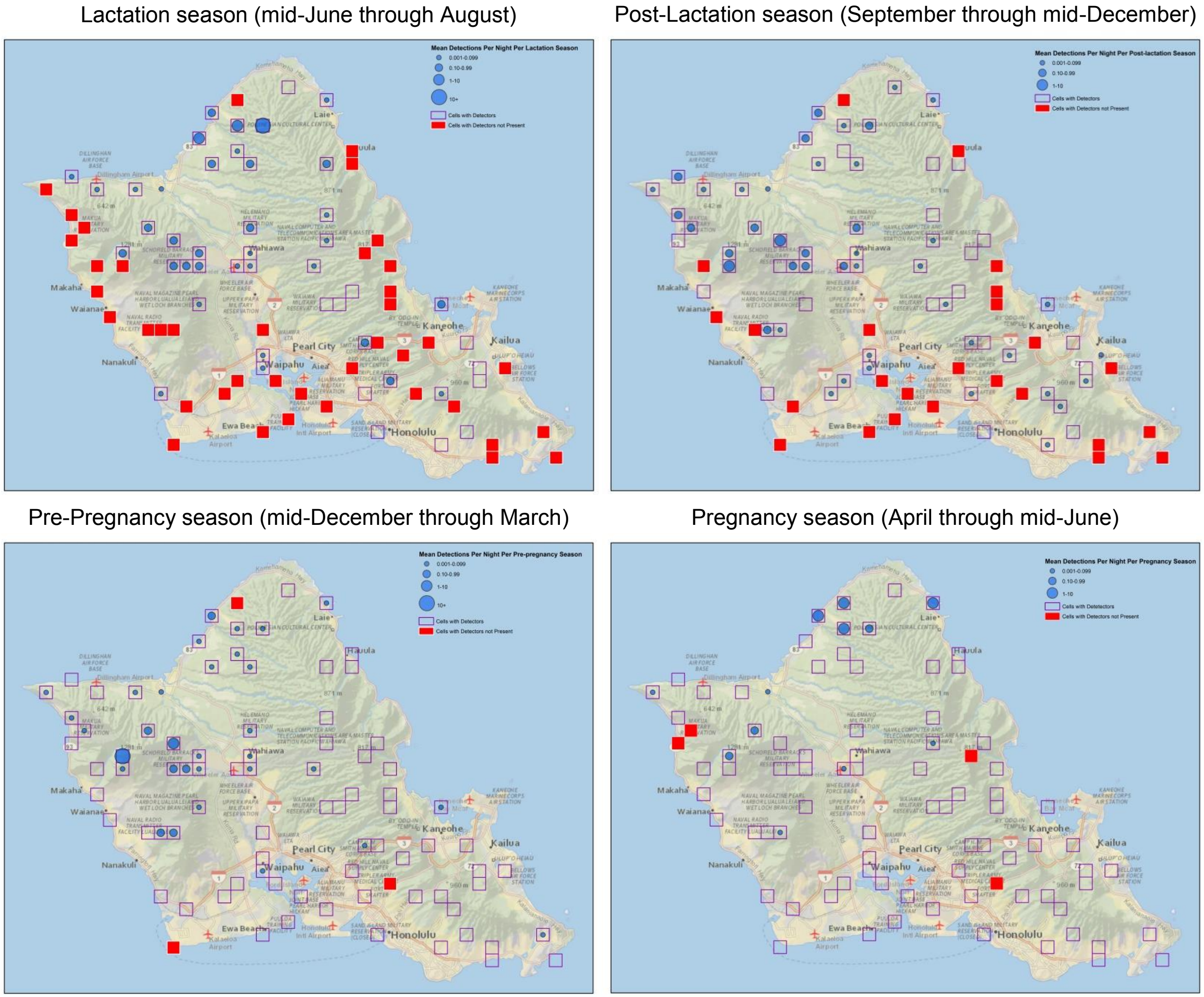

Figure 6a: Mean detections per night by site and season. June 2017 – June 2018.

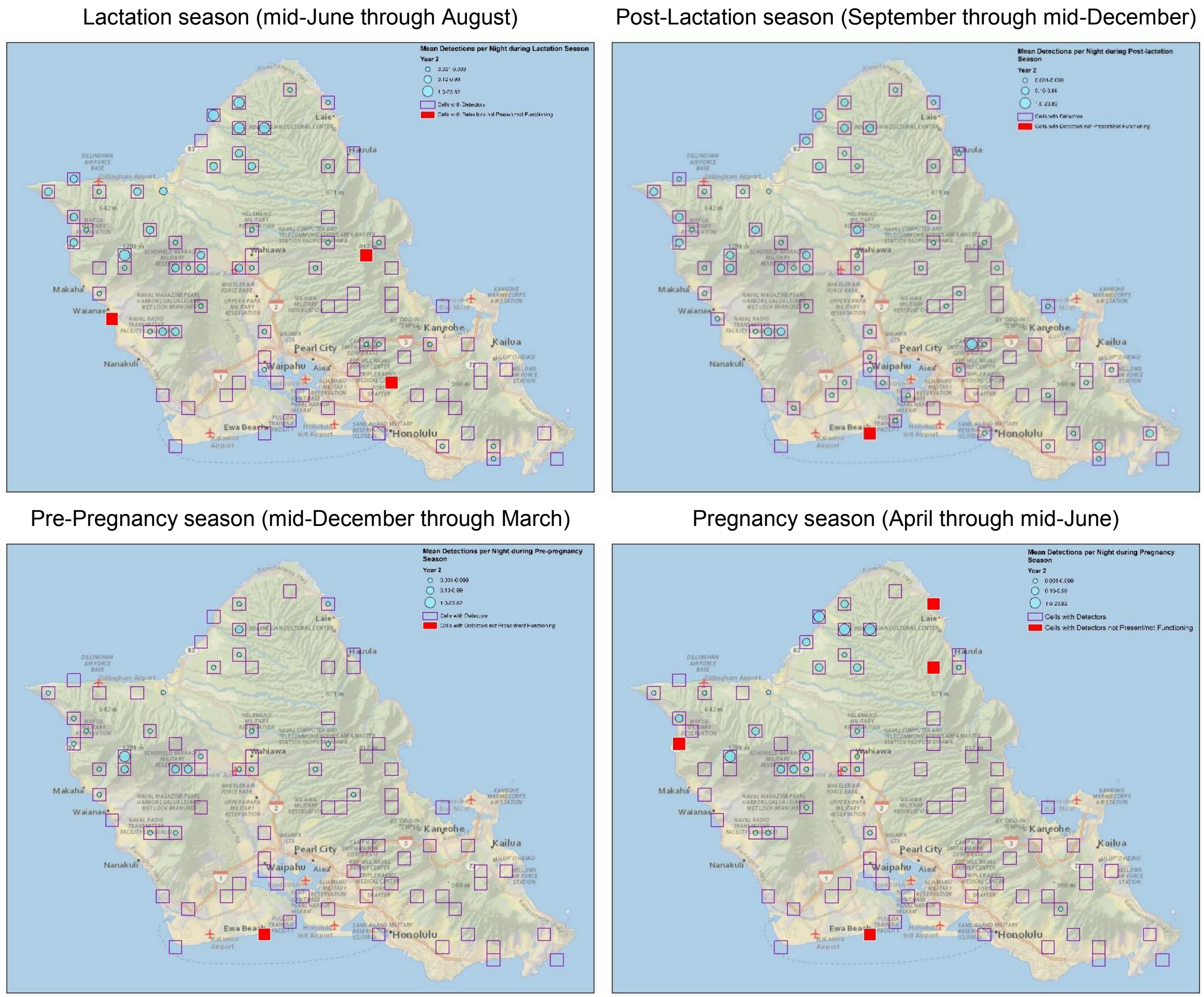

Figure 6b: Mean detections per night by site and season. June 2018 – June 2019.

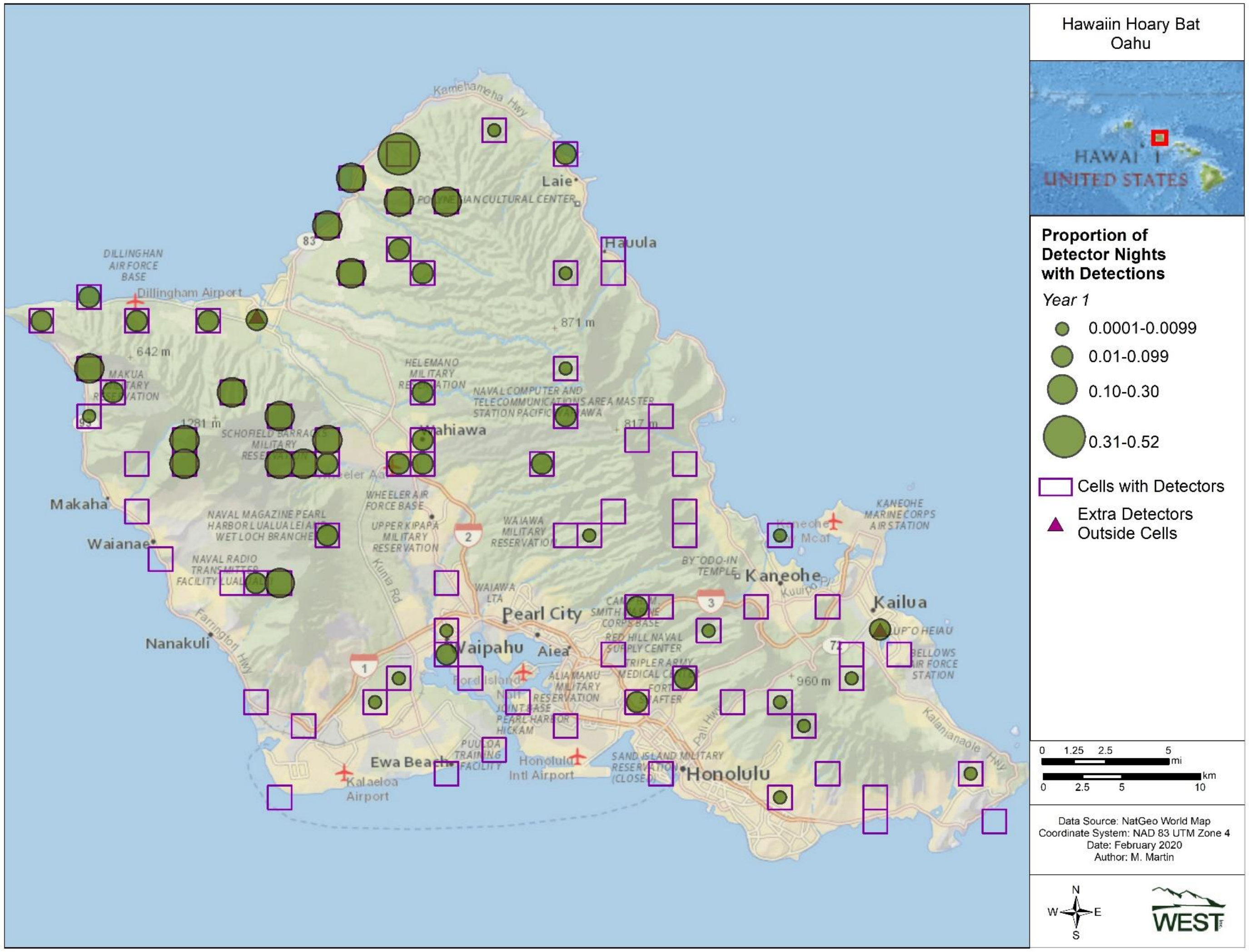

Figure 7a: Proportion of nights with detections by site between June 2017 and June 2018.

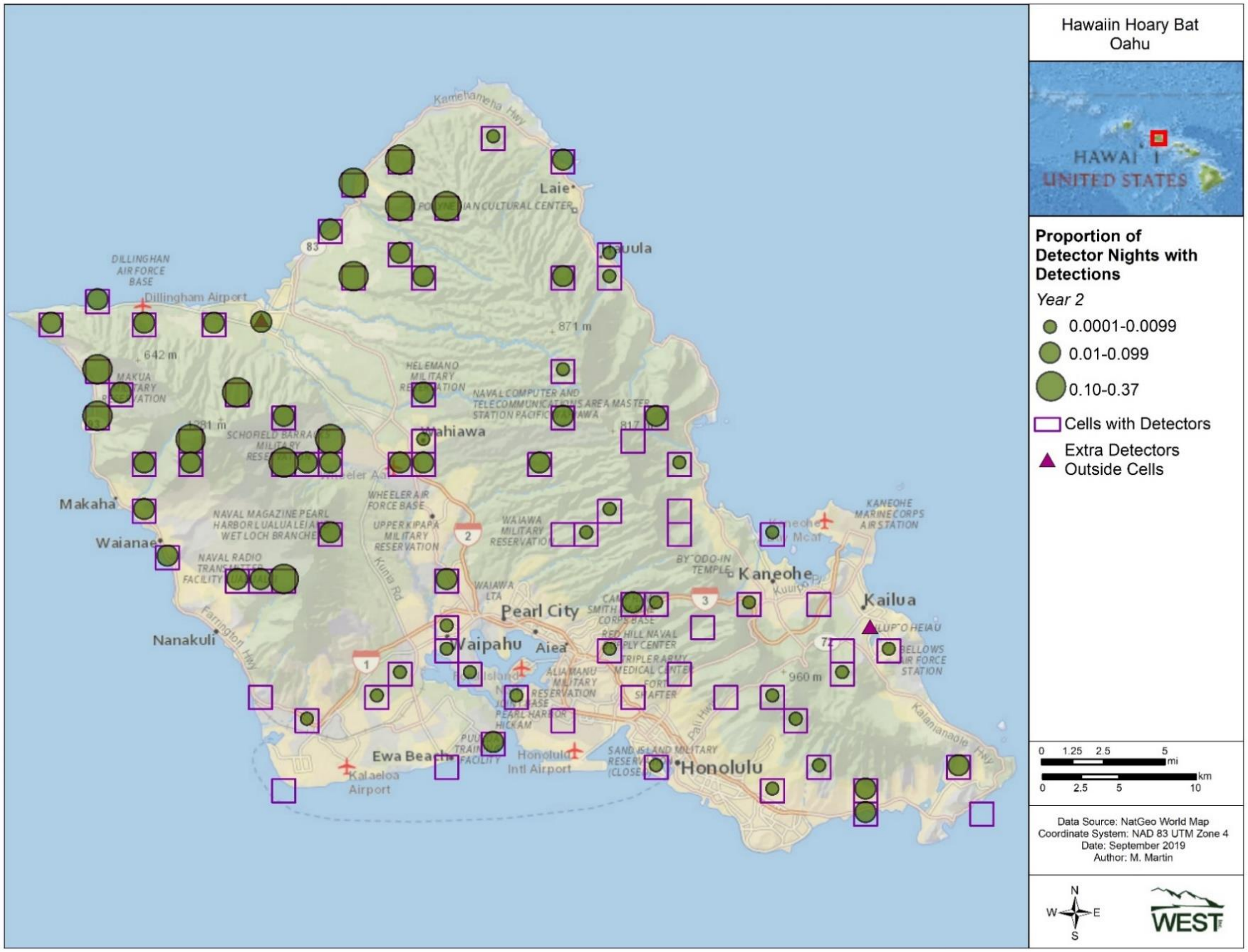

Figure 7b: Proportion of nights with detections by site between June 2018 and June 2019.

Lactation season (mid-June through August)

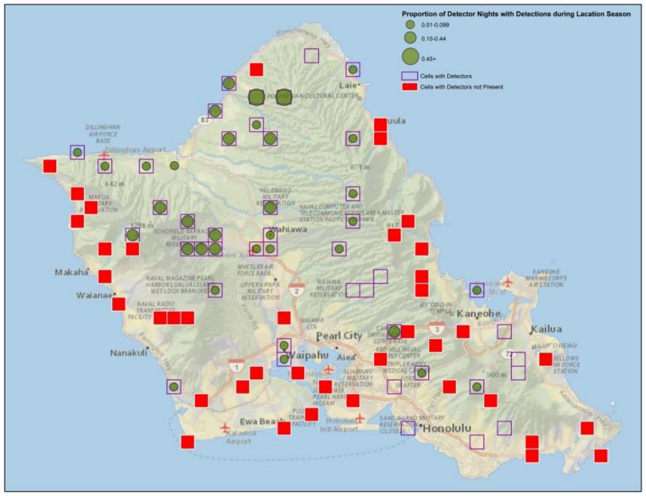

Post-Lactation season (September through mid-December)

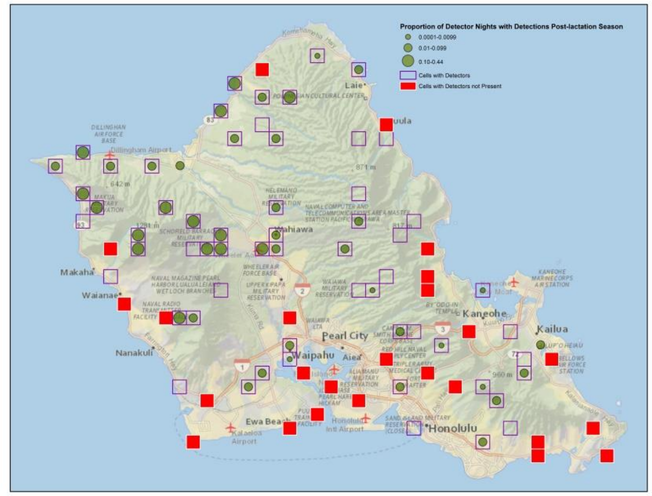

Pre-Pregnancy season (mid-December through March)

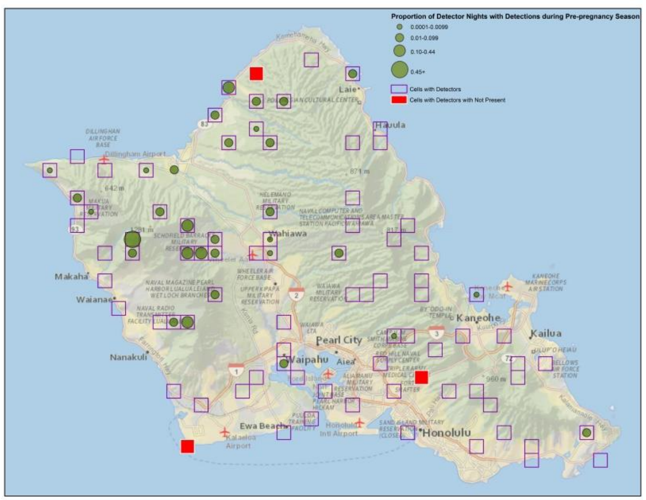

Pregnancy season (April through mid-June)

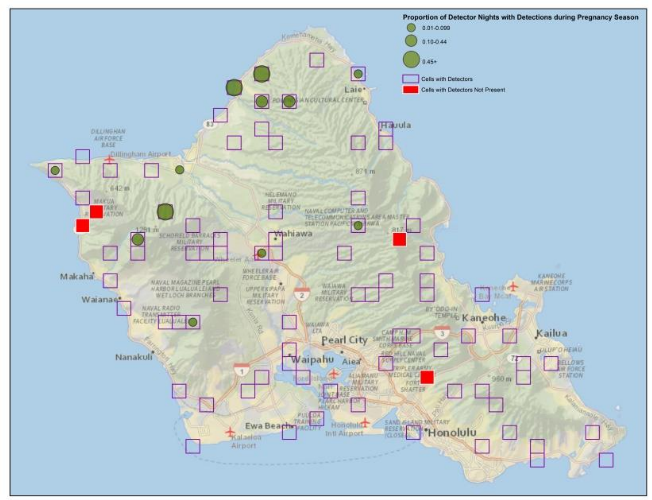

Figure 8a: Proportion of detector nights with detections by site and season between June 2017 and June 2018.

Lactation season (mid-June through August)

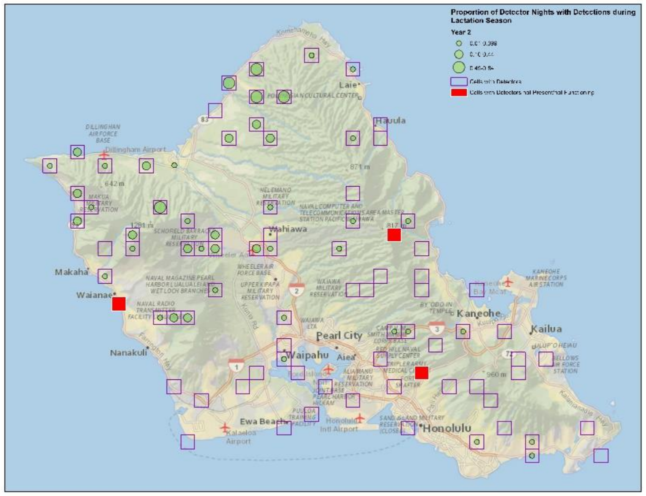

Post-Lactation season (September through mid-December)

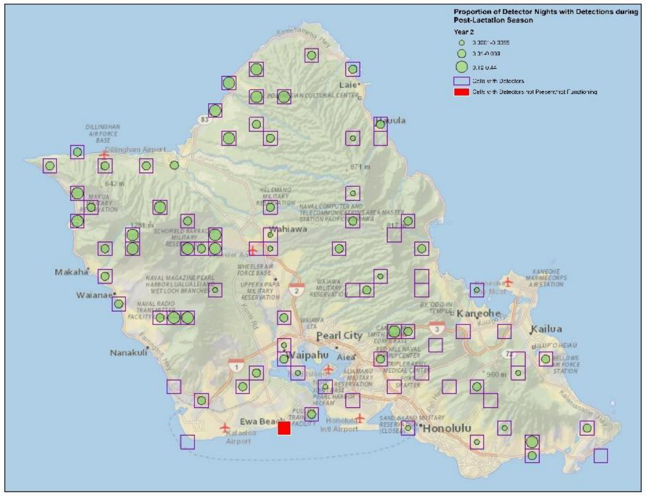

Pre-Pregnancy season (mid-December through March)

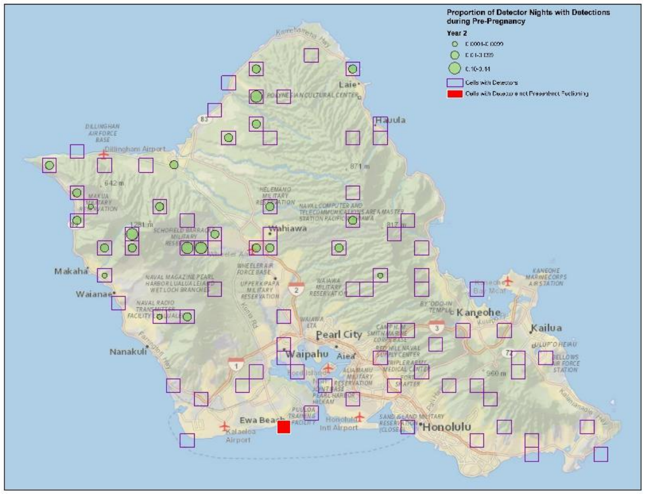

Pregnancy season (April through mid-June)

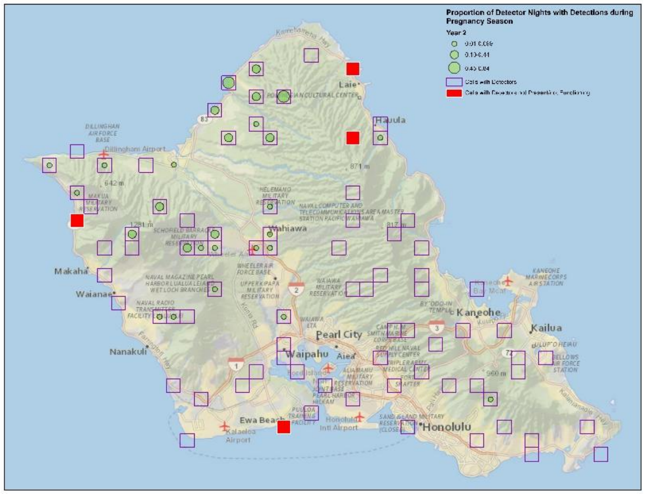

Figure 8b: Proportion of detector nights with detections by site and season between June 2018 and June 2019.

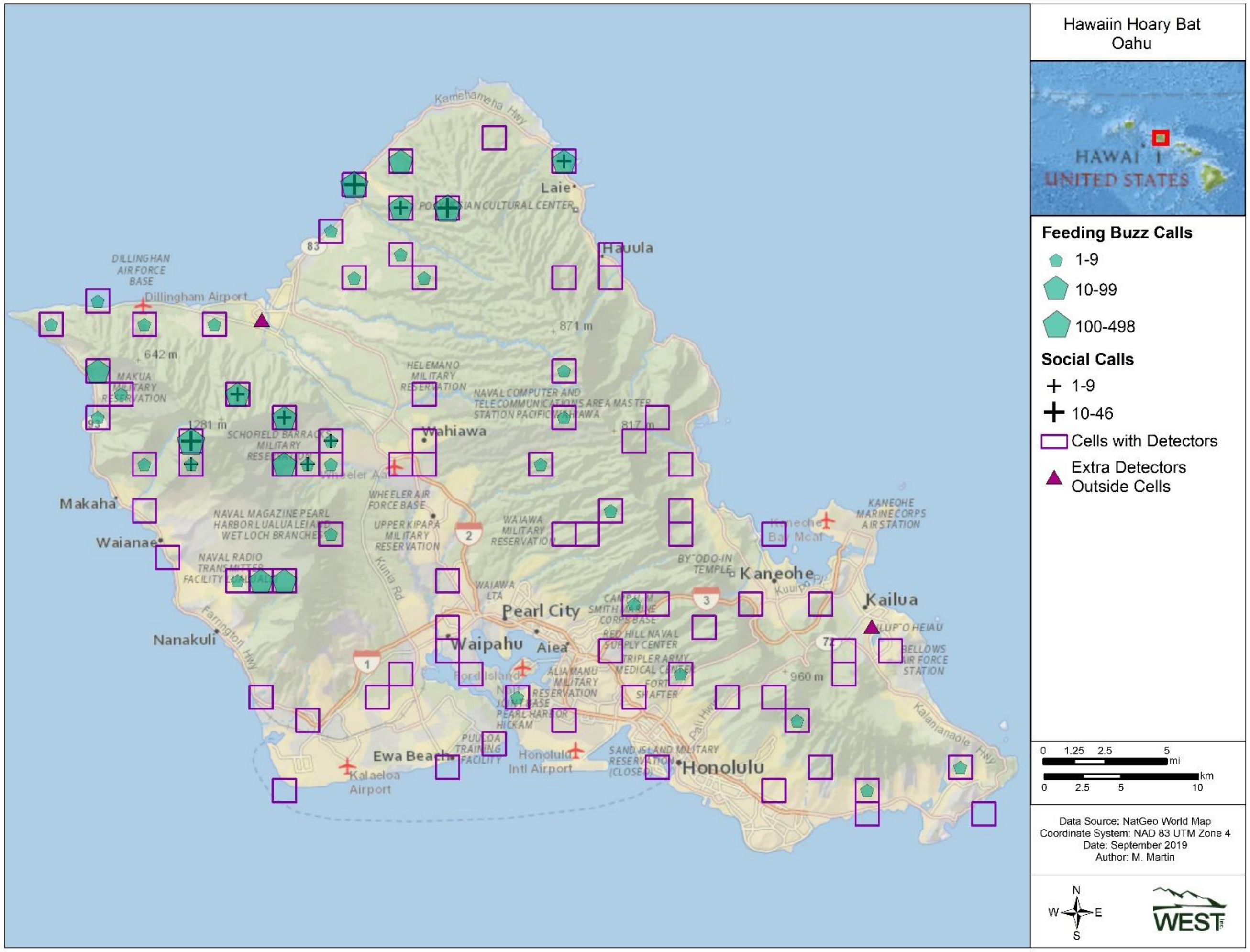

Figure 9: Distribution of feeding buzzes and social calls recorded between June 2017 and October 2019.

Occupancy modeling

The sample data available as of October 2019 were examined in an occupancy analysis to obtain estimates of occupancy and detection rates. The results presented herein are preliminary and are for informational purposes only. The results should not be cited outside of project planning discussions or without permission of the authors. We begin with an assessment of the assumptions for occupancy modeling, report the results of the occupancy modeling exercise, and determine if the current sample size of detectors is sufficient to meet the goal of estimating the HAHOBA occupancy rate on Oahu.

The independence of nightly detection data was evaluated by applying join count chi square tests of adjacent survey nights to data sets obtained by systematically sampling the nightly detector data every 7th, 10th, 14th, and 21st night. We attempted to apply the test to the nightly data and data systematically selected every four days, but the dimension of the resulting data set was often too large to process. In the cases where the join count test ran successfully for 4-day interval data, the test result indicated correlated data. For all data subsets, the join count test was conducted independently by reproductive season and year, assuming an independent detection model and a correlated detection model.

Small p-values from the join count test indicate the number of adjacent temporal joins exceeded the expectation under the independence assumption (Table 2). The assumption of independence resulted in a poor fit for at least one season in all subsample data sets. Based on the results of the join count tests for the independent detection model, we assume temporal correlation is substantial when examining detections from every data subset. We found the correlated detections model adequately accounted for the correlation between adjacent detections for a subsampling interval of seven days for the post-lactation, pre-pregnancy, and pregnancy breeding seasons. However, an interval of 14 days was required to adequately model detections in the lactation season. To both meet the assumptions of the correlated detections occupancy model and retain as much detection data as possible for precise estimation, the dataset used for occupancy modeling was developed using an interval of seven days for the post-lactation, pre-pregnancy, and pregnancy breeding seasons, and an interval of 14 days for the lactation season.

Table 2: Join count test results for two models (independent detection or correlated detections), four seasons, and four sampling intervals across three survey years.

Season	Interval (days)	Model	Year 1		Year 2		Year 3	
			Join count χ^2	p-value	Join count χ^2	p-value	Join count χ^2	p-value
Lactation	7	Ind.	46.52	0.007	9,7493.79	<0.001	225.04	<0.001
	10	Ind.	2032.34	<0.001	59.30	0.002	23.89	0.012
	14	Ind.	11.93	0.039	10.67	0.038	17.06	0.018
	21	Ind.	3.71	0.181	2.93	0.303	21.24	0.011
Post-Lactation	7	Ind.	35.92	0.005	14.81	0.029	-	-
	10	Ind.	26.09	0.010	11.01	0.032	-	-
	14	Ind.	4.97	0.155	3.00	0.149	-	-
	21	Ind.	0.32	0.806	4.26	0.066	-	-

Table 2: Join count test results for two models (independent detection or correlated detections), four seasons, and four sampling intervals across three survey years.

Season	Interval (days)	Model	Year 1		Year 2		Year 3	
			Join count χ^2	p-value	Join count χ^2	p-value	Join count χ^2	p-value
Pre-Pregnancy	7	Ind.	7.42	0.097	0.07	0.966	-	-
	10	Ind.	29.09	0.005	1.82	0.308	-	-
	14	Ind.	1.30	0.622	0.27	0.739	-	-
	21	Ind.	3.79	0.089	1.27	0.891	-	-
Pregnancy	7	Ind.	55.26	0.003	23.25	0.007	-	-
	10	Ind.	5.62	0.197	3.27	0.233	-	-
	14	Ind.	7.14	0.089	0.55	0.832	-	-
	21	Ind.	1.29	0.803	1.38	0.476	-	-
Lactation	7	Corr.	13.89	0.029	699.87	0	23.75	0.024
	10	Corr.	146.86	<0.001	11.65	0.062	8.73	0.190
	14	Corr.	5.50	0.145	4.82	0.144	4.19	0.267
	21	Corr.	1.38	0.475	2.83	0.194	9.10	0.024
Post-Lactation	7	Corr.	4.06	0.436	1.28	0.906	-	-
	10	Corr.	5.56	0.152	2.15	0.627	-	-
	14	Corr.	2.09	0.395	0.94	0.402	-	-
	21	Corr.	0.30	0.590	4.22	0.054	-	-
Pre-Pregnancy	7	Corr.	2.79	0.893	0.08	0.367	-	-
	10	Corr.	7.73	0.094	0.94	0.415	-	-
	14	Corr.	1.51	0.382	0.49	0.694	-	-
	21	Corr.	1.65	0.303	1.54	0.848	-	-
Pregnancy	7	Corr.	10.48	0.187	4.82	0.417	-	-
	10	Corr.	2.32	0.625	2.28	0.313	-	-
	14	Corr.	3.69	0.412	0.43	0.880	-	-
	21	Corr.	0.21	0.990	0.81	0.715	-	-

Ind. = independent detection; Corr. = correlated detections.

Site-level covariates (Table 3) were used to model occupancy, local extinction and colonization, and the probability of local presence in an occupied site just prior to the first survey period. Site-level covariates included the human population per square mile (US Census Bureau 2019), mean elevation of the grid cell in meters (USGS 2017), and the percentage of the grid cell covered in tree-dominated land cover classes (Landfire Existing Vegetation Type 2017). Each of the three site-level covariates was also discretized into a 2-level category of low/high based on the median value and are indicated as covariates ending in "Class."

Table 3: Site-level covariates for occupancy modeling

Site-level Covariate	Description
PopSqMi	Human population per square mile (mi) in each grid cell.
PopSqMiClass	0 if population density <64.60 people per square mi, 1 otherwise.
Elev	Mean site elevation in meters in each grid cell.
ElevClass	0 if Elevation <141.43 m, 1 otherwise.
PctTrees	Percent tree cover in grid cell.
PctTreesClass	0 if percent tree cover <20.68%, 1 otherwise.

The dynamic occupancy model for correlated detections was then applied to the subsampled detection data set and covariates were examined in a model selection process. Local extinction and colonization parameters were modeled by season, but these models did not converge. Visit-level and coarser covariates (season- and site-level) were used to model detection probabilities. Visit-level covariates included the month of the survey and the microphone model used with the bat detector. Microphones were swapped between February and June of 2019. To avoid confounding effects of microphone and season, microphone model effects will be omitted from detection probability models until a full year of data has been collected with the SMM-U2 microphone. Model parameters are defined in Table 4, and the results of the modeling exercise are provided in Table 5 for the subset of models that converged.

Table 4: Occupancy parameters for the multi-season dynamic occupancy model for correlated detections (Hines et al. 2014)

Occupancy Model Parameter	Description
psi	Occupancy rate.
th0	Probability the species is available at a survey occasion given the site is occupied and the species was **not** available at the previous survey occasion.
th1	Probability the species is available at a survey occasion given the site is occupied and the species **was** available at the previous survey occasion.
gam	Probability a site not occupied during a given season is colonized during the next season.
eps	Probability a site occupied during a given season is not occupied during the next season.
p	Probability a species is detected given the site is occupied and the species is currently available.
th0pi	Probability a site is occupied and the species is available just prior to the first survey occasion.

Table 5: Occupancy modeling results for the multi-season dynamic occupancy model for correlated detections

Model	AIC	Delta AIC	AIC wgt	no. Par.
psi,th0(),th1(),gam(),eps(),p(Season),th0pi(PopSqMiClass)	2120.24	1.06	0.3031	11
psi,th0(),th1(),gam(),eps(),p(Season),th0pi(PopSqMi)	2123.64	4.46	0.0554	11
psi,th0(),th1(),gam(2SeasonPostLact),eps(2SeasonPostLact),p(),th0pi()	2123.82	4.64	0.0506	9
psi,th0(),th1(),gam(),eps(),p(),th0pi(PopSqMiClass)	2125.82	6.64	0.0186	8
psi(ElevMn)th0(),th1(),gam(),eps(),p(Season),th0pi()	2126.72	7.54	0.0119	11
psi(PopSqMiClass)th0(),th1(),gam(),eps(),p(Season),th0pi()	2127.10	7.92	0.0098	11
psi(ElevMn)th0(),th1(),gam(PctTreesClass),eps(PctTreesClass),p(Season),th0pi()	2127.23	8.05	0.0092	13
psi(PopSqMi)th0(),th1(),gam(),eps(),p(Season),th0pi()	2127.93	8.75	0.0065	11
psi,th0(),th1(),gam(),eps(),p(Season),th0pi()	2129.21	10.03	0.0034	10
psi,th0(),th1(),gam(),eps(),p(Season),th0pi(PctTreesClass)	2129.26	10.08	0.0033	11
psi(ElevMn)th0(),th1(),gam(PopSqMiClass),eps(PopSqMiClass),p(Season),th0pi()	2129.39	10.21	0.0031	13
psi,th0(),th1(),gam(PctTreesClass),eps(PctTreesClass),p(Season),th0pi()	2130.01	10.83	0.0023	12
psi(PctTrees)th0(),th1(),gam(),eps(),p(Season),th0pi()	2130.86	11.68	0.0015	11
psi(PctTreesClass)th0(),th1(),gam(),eps(),p(Season),th0pi()	2131.14	11.96	0.0013	11
psi(ElevClass)th0(),th1(),gam(),eps(),p(Season),th0pi()	2131.21	12.03	0.0013	11
psi,th0(),th1(),gam(),eps(),p(Season),th0pi(ElevClass)	2132.96	13.78	0.0005	11
psi(PopSqMiClass),th0(),th1(),gam(),eps(),p(),th0pi()	2142.94	23.76	0	8
psi,th0(),th1(),gam(),eps(),p(Month),th0pi()	2144.03	24.85	0	8
psi,th0(),th1(),gam(),eps(),p(),th0pi()	2145.26	26.08	0	7
psi,th0(),th1(),gam(PctTreesClass),eps(PctTreesClass),p(),th0pi()	2145.67	26.49	0	9
psi,th0(),th1(),gam(),eps(),p(),th0pi(PctTreesClass)	2145.69	26.51	0	8
psi,th0(),th1(),gam(PopSqMiClass),eps(PopSqMiClass),p(),th0pi()	2146.79	27.61	0	9
psi(PctTreesClass),th0(),th1(),gam(),eps(),p(),th0pi()	2147.20	28.02	0	8

AIC = Akaike Information Criterion; wgt = weight; no. Par. = no parameter.

The top model based on Akaike Information Criterion described detection probabilities by reproductive season and the initial probability HAHOBA was locally present prior to the first survey as a function of low or high human population density (see Appendix A for PRESENCE model output). Occupancy estimates were modeled as stable over the full survey period and ranged from 0.4317 to 0.4465 (Table 6, Figure 10). The probability HAHOBA was locally present at an occupied grid cell just prior to the first survey was 0.2062 (Standard Error [SE] = 0.0665, 95% confidence interval [CI]: 0.1048, 0.3654) for cells with high human population density and 0.6042 (SE = 0.1277, 95% CI: 0.3489, 0.8130) for cells with low human population density. The probability HAHOBA was locally present at an occupied site given the species was locally present in the previous survey occasion was estimated to be 0.8241 (SE = 0.0354, 95% CI: 0.7437, 0.8833). The probability of local presence at an occupied site where the species was not locally present in the previous survey occasion was 0.0623 (SE = 0.0142, 95% CI: 0.0396, 0.0967). The estimated detection probabilities conditional on local presence varied by season (Table 6, Figure 11) and ranged from 0.25 in the pre-pregnancy season to 0.53 in the lactation season.

Table 6: Estimates of occupancy and detection rates for the top multi-season dynamic occupancy model for correlated detections.

Year	Season	Est. Occupancy Rate	SE	95% CI	Est. Detection Probability Given Local Presence	SE	95% CI
1	Lactation	0.4465	0.0951	(0.2750, 0.6317)	0.5347	0.0795	(0.3806, 0.6825)
1	Post-Lactation	0.4435	0.0798	(0.2872, 0.5999)	0.3977	0.0485	(0.3076, 0.4954)
1	Pre-Pregnancy	0.4410	0.0693	(0.3051, 0.5769)	0.2500	0.0485	(0.1673, 0.3562)
1	Pregnancy	0.4388	0.0635	(0.3145, 0.5632)	0.4204	0.0655	(0.2998, 0.5512)
2	Lactation	0.4370	0.0614	(0.3167, 0.5573)	0.5347	0.0795	(0.3806, 0.6825)
2	Post-Lactation	0.4354	0.0620	(0.3138, 0.5570)	0.3977	0.0485	(0.3076, 0.4954)
2	Pre-Pregnancy	0.4340	0.0644	(0.3078, 0.5601)	0.2500	0.0485	(0.1673, 0.3562)
2	Pregnancy	0.4328	0.0676	(0.3004, 0.5652)	0.4204	0.0655	(0.2998, 0.5512)
3	Lactation	0.4317	0.0710	(0.2925, 0.5710)	0.5347	0.0795	(0.3806, 0.6825)

Est. = estimated; SE = Standard Error; CI = confidence Interval.

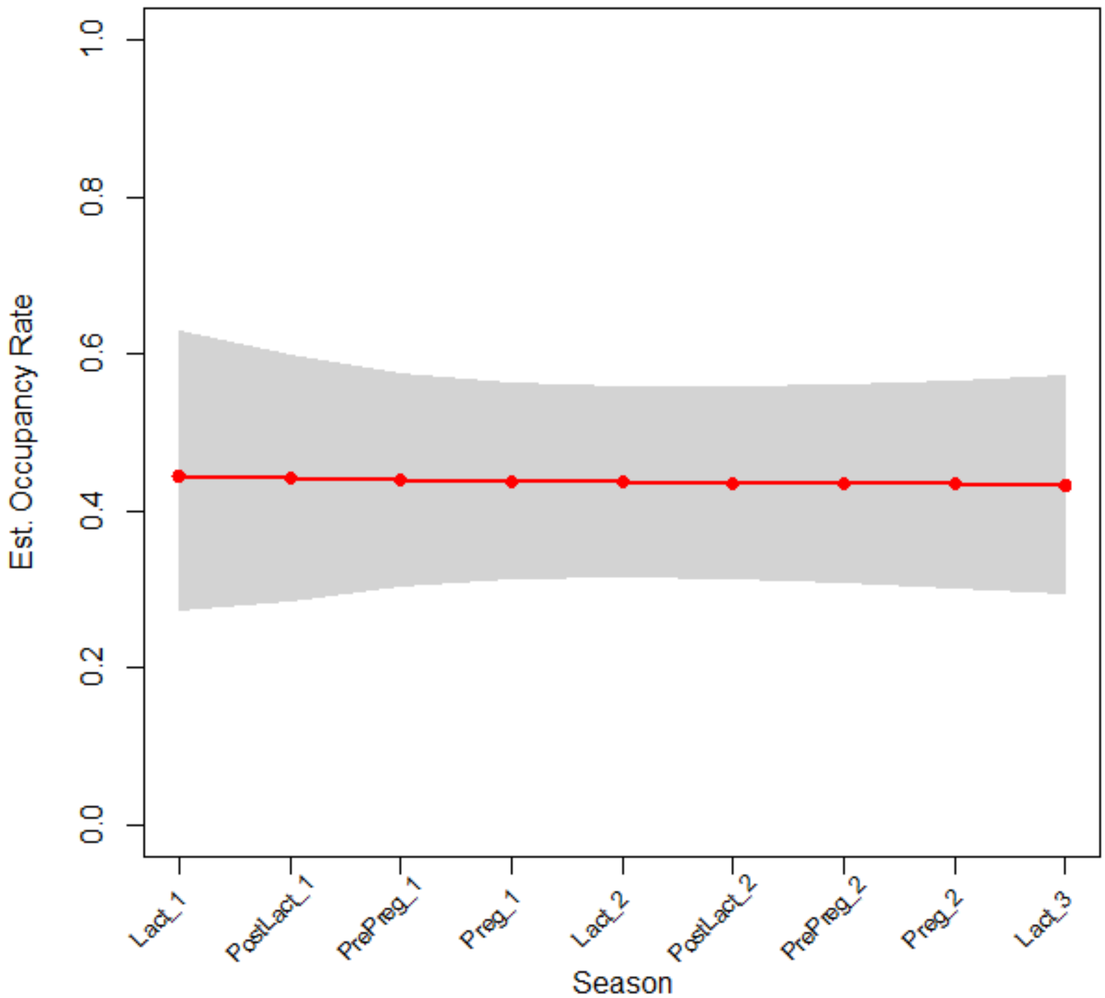

Figure 10: Occupancy estimates and 95% confidence bands by reproductive season and year.

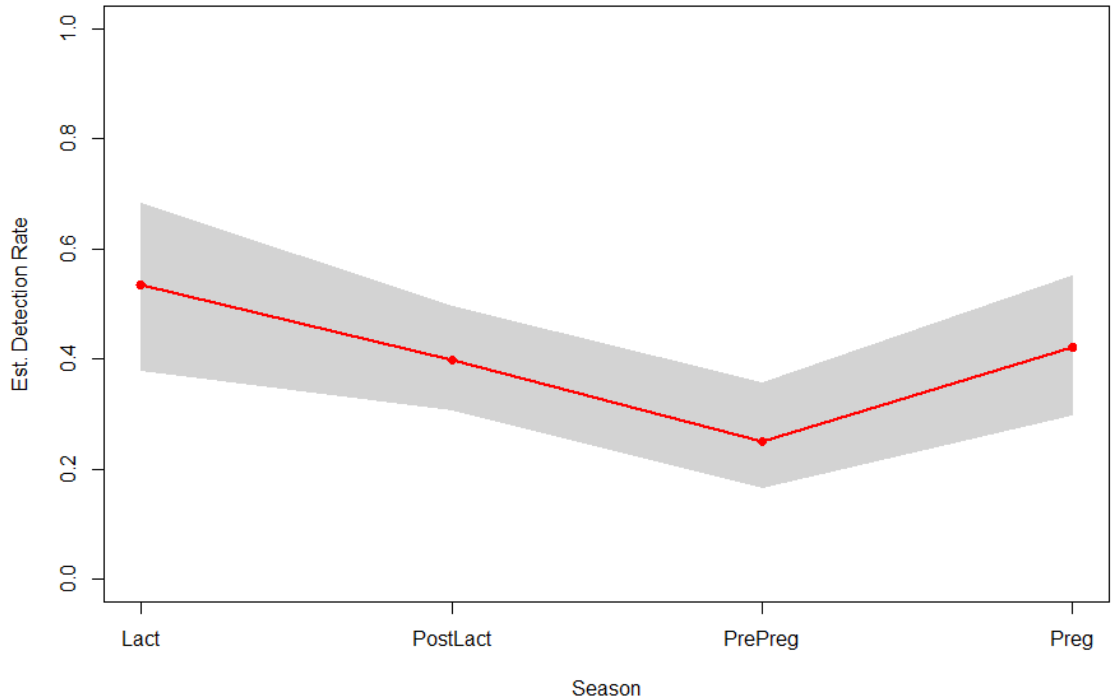

Figure 11: Detection probability estimates and 95% confidence bands by reproductive season.

DISCUSSION

Temporal correlation among detections violates assumptions of independent detections required for standard occupancy modeling. Failure to account for temporal correlation may result in variance underestimation leading to narrow CIs and inappropriately small p-values that indicate a significant effect when none exists. One approach to obtaining independent detections is to reduce the detector nights to a subset of data for which independent detections may be assumed (Wright et al. 2016). Removing detection occasions reduces the sample size of observations, which may make modeling with covariates more difficult. Data reduction may also eliminate incidental detections of HAHOBA that may simply be transiting through a grid cell and not truly occupying the cell for biological reasons, therefore, helping to better address occupancy for grid cells with consistent use. Another approach to address temporal correlation is to implement detection models that apply a first-order Markov process (Hines et al. 2014) to account for temporal correlation. To retain the most data while still meeting the assumptions of independent detections, we subsampled detections recorded every 14 days for the Lactation season and every seven days for the Post-Lactation, Pre-Pregnancy, and Pregnancy seasons and then applied the occupancy model that accounted for correlated detections.

The final occupancy model for our data set assumed closure within each reproductive season, modeled the local colonization and extinction rates as equal across all seasons, and modeled detection by season. Occupancy models describing the extinction and colonization parameters by season did not converge, likely because there are only two replications of each seasonal transition so far (e.g., Lactation to Post-lactation in each of two years). HAHOBA distribution appears to vary by season (Figures 6a, 6b, 8a, and 8b), with the largest extent of the distribution occurring in the Post-Lactation period. These seasonal differences could be explained by changing occupancy or by changes in the detectability of the species across the reproductive seasons. Additional seasonal data may provide more information to assess how occupancy, rather than detection, might change by season. Bayesian analysis may also provide tools to determine if seasonal differences are due to detection differences, distributional changes, or a mixture of both.

Given this study is at roughly the halfway point, an assessment of current effort is warranted. Over two years of data have been collected on HAHOBA distribution and occupancy. At the request of the ESRC, the original sample frame included all grid cells that contained some land area that could provide a sample site for a detector, even if the majority of the cell was over open water (i.e., offshore). This was done to not exclude possible sampling along the coastline. Three detectors were located in cells in beach parks or close to the waterfront in cells mostly (over 85%) represented by open water conditions (see grid cells 110, 112, and 113 in Figure 2). Two of the three cells have had zero detections in more than two years of surveys, while the third has had only five detections over four separate nights (Table 7). Due to the large amount of open water in these three cells, the detector sample sites are not considered representative of the cell, therefore, potentially limiting their contribution to future analyses focused on habitat associations. While the data collected to date in these cells will continue to be used in future analyses of bat distribution and occupancy across the island, we suggest data collection from these detectors could be discontinued at this time. We also plan to cease collecting data at the two non-random detectors (999-Hamakua Ponds and 000 Goodale Tribe) and consider ceasing monitoring of the Kipapa North Fence (Site-073) detector, which is located on a difficult to access ridge along the Koʻolau crest that is regularly inundated with clouds, rarely accessible, and as a result, missing large amounts of data (i.e., only 270 detector nights of data out of more than 700 possible nights). Data from all six of these sites can still be incorporated into analyses, as appropriate, for the time periods in which they were operating. However, we feel resources saved by ceasing data collection at these sites can be better used on analysis or other needs while not compromising the occupancy study.

MacKenzie's (2006) recommendation on survey designs for assessing habitat use when detection probabilities are less than one is to select a single sample and revisit the same sites over time. This survey design provides a basis to estimate the detection probability without confounding habitat and detection variables. Because the detection probability in our study is estimated to be well below one, we recommend continued monitoring of all detectors except those six noted above at their current locations in order to provide the most appropriate data set for incorporating habitat variables into the occupancy analysis.

Table 7. Sites and site characteristics for detectors with five or fewer detections for full time period (June 2017 through October 2019).

Site ID	Site Name	Detections	Elevation (m)	% Tree Cover	Human Population per Square Mile
Site-006	006 Waihee Res	0	131.28	57.8	402.47
Site-008	008 Ewa Beach Park	0	0.28	0.4	3760.29
Site-026	026 Kapaa Kawainui	0	74.42	23.7	1265.63
Site-032	032 Nuuanu Watershed	0	244.36	61.6	1086.93
Site-040	040 Hickham AFB	0	2.46	0.0	2834.81
Site-072	072 Waihee Wells	0	227.86	79.7	171.94
Site-073	073 Kipapa North Fence	0	421.22	94.9	22.55
Site-088	088 Kawainui Marsh 1	0	42.12	30.9	1658.75
Site-110	110 Halone Blowhole	0	0.37	0.1	0
Site-112	112 Barbers point	0	0.14	0.9	0
Site-030	030 Sacred Falls	1	30.21	37.5	453.92
Site-038	038 Moanalua Trail	1	314.4	96.6	105.03
Site-068	068 Waikane Valley	1	35.85	50.4	210.07
Site-078	078 Sand Island	1	0.69	1.0	32.55
Site-090	090 Kaau Crater Trail	1	315.74	92.0	713.35
Site-114	114 Waipio Soccer Complex	1	5.78	31.5	35.87
Site-034	034 Barbers Point Res	2	33.45	5.0	205.56
Site-043	043 Manana Trail 1	2	260.56	90.7	22.13
Site-044	044 Royal Hawaiian Golf	2	122.30	57.8	97.02
Site-054	054 Anchor Church	2	202.05	52.8	1369.65
Site-059	059 Moanalua Red Hill	2	76.12	4.2	2549.10
Site-106	106 Puu Pia Trail	2	404.42	97.3	77.82
Site-113	113 Hauula District Park	2	1.19	2.5	1126.76
Site-024	024 Ft Shafter	3	18.26	1.1	2586.92
Site-036	036 Kroc Center	3	25.95	0.0	355.17
Site-031	031 Plantation Village	4	17.73	4.5	13758.98
Site-058	058 Kailua Heights Res	4	34.51	2.0	6466.12
Site-077	077 Manana Trail 2	4	329.33	97.0	10.19
Site-084	084 Aiea Loop Ridge	4	307.80	89.3	0
Site-102	102 Pearl Harbor	4	2.20	0.4	281.00
Site-050	050 HECO Kahe Point	5	36.43	1.6	565.41
Site-100	100 Heeia State Park	5	0.06	0.3	5.96

REFERENCES

Fiske, I. J. and R. B. Chandler. 2011. Unmarked: An R Package for Fitting Hierarchical Models of Wildlife Occurrence and Abundance. Journal of Statistical Software 43(10): 1-23. doi: 10.18637/jss.v043.i10.

Gorressen, M. P., F. J. Bonaccorso, C. A. Pinzari, C. M. Todd, K. Montoya-Aiona, and K. Brinck. 2013. A Five-Year Study of Hawaiian Hoary Bat (*Lasiurus cinereus Semotus*) Occu Pancy on the Island of Hawai`I. Technical Report HCSU-041. Hawai`i Cooperative Studies Unit. 2 U.S. Geological Survey, Pacific Island Ecosystems Research Center, Kīlauea Field Station. July, 2013. Available online: https://hilo.hawaii.edu/hcsu/documents/TR41_Gorresen_Bat_occupancy.pdf

Hines, J. E., J. D. Nichols, J. A. Royle, D. I. MacKenzie, A. M. Gopalaswamy, N. S. Kumar, and K. U. Karanth. 2010. Tigers on Trails: Occupancy Modeling for Cluster Sampling. Ecological Applications 20(5): 1456-1466.

Hines, J. E., J. D. Nichols, and C. J. A. 2014. Multiseason Occupancy Models for Correlated Replicate Surveys. Methods in Ecology and Evolution 5: 583-591 pp. doi: 10.1111/2041-210X.12186. Available online: https://besjournals.onlinelibrary.wiley.com/doi/pdf/10.1111/2041-210X.12186

LANDFIRE. 2017. Existing Vegetation Type Layer. Landscape Fire and Resource Management Planning Tools Project (LANDFIRE). Department of the Interior (DOI) US Geological Survey (USGS). Last modified February 2017. Information available online at: http://landfire.cr.usgs.gov/viewer/

MacKenzie, D. I. 2006. Modeling the Probability of Resource Use: The Effect of, and Dealing with, Detecting a Species Imperfectly. Journal of Wildlife Management 70(2): 367-374. doi: 10.2193/0022-541x(2006)70[367:mtporu]2.0.co;2.

MacKenzie, D. I., J. D. Nichols, J. A. Royle, K. H. Pollock, L. L. Bailey, and J. E. Hines. 2006. Occupancy Estimation and Modeling: Inferring Patterns and Dynamics of Species Occurrence. Academic Press, Elsevier, Burlington, Massachusetts.

Menard, T. 2001. Activity Patterns of the Hawaiian Hoary Bat (*Lasiurus cinereus Semotus*) in Relation to Reproductive Time Periods. MSc Thesis. Univeristy of Hawaii. Available online: https://www.opeapea.org/paper-blog/2019/2/2/Activity%20patterns%20of%20the%20Hawaiian%20hoary%20bat%20(Lasiurus%20cinereus%20semotus)%20in%20relation%20to%20reproductive%20time%20periods.%20MSc%20Thesis,%20University%20of%20Hawaii.

National Geographic Society (National Geographic). 2018. World Maps. Digital topographic map. PDF topographic map quads. Accessed March 8, 2018. Available online: http://www.natgeomaps.com/trail-maps/pdf-quads

National Geographic Society (National Geographic). 2020. World Maps. Digital topographic map. PDF topographic map quads. Accessed January 2020. Available online: http://www.natgeomaps.com/trail-maps/pdf-quads

North American Datum (NAD). 1983. NAD83 Geodetic Datum.

R Development Core Team. 2016. R: A Language and Environment for Statistical Computing. R Foundation for Statistical Computing, Vienna, Austria. Information online: http://www.R-project.org/

Stevens, D. L., Jr. and A. R. Olsen. 2003. Variance Estimation for Spatially Balanced Samples of Environmental Resources. Environmetrics 14(6): 593-610 pp. doi: 10.1002/env.606. Available online: https://onlinelibrary.wiley.com/doi/abs/10.1002/env.606

Stevens, D. L., Jr. and A. R. Olsen. 2004. Spatially Balanced Sampling of Natural Resources. Journal of the American Statistical Association 99(465): 262-278. doi: 10.1198/016214504000000250.

US Census Bureau. 2019. 2010 Census - Block Maps. Last update: March 14, 2019. Accessed January 2020. Available online: https://www.census.gov/geographies/reference-maps/2010/geo/2010-census-block-maps.html

US Geological Survey (USGS). 2017. USGS National Elevation Dataset (NED). State of North Dakota, State Water Commission. Last updated February 27, 2019. Information online: https://catalog.data.gov/dataset/usgs-national-elevation-dataset-ned

US Geological Survey (USGS). 2019. PRESENCE Version 12.37- Software to Estimate Patch Occupancy and Related Parameters. Accessed January 2020. Information online: https://www.mbr-pwrc.usgs.gov/software/presence.html

Wildlife Acoustics, Inc. 2019. Kaleidoscope Pro® Version 5.1.0. (Acoustic analysis computer software). Wildlife Acoustics, Maynard, Massachusetts. Information online: www.wildlifeacoustics.com

Wright, W. J., K. M. Irvine, and T. J. Rodhouse. 2016. A Goodness-of-Fit Test for Occupancy Models with Correlated within-Season Revisits. Ecology and Evolution 6(15): 5404-5415 pp. doi: 10.1002/ece3.2292. Available online: https://onlinelibrary.wiley.com/doi/full/10.1002/ece3.2292

Appendix A: Output of Final Occupancy Model

```
PRESENCE - Presence/Absence-Site Occupancy data analysis
Wed Jan 15 12:00:25 2020,       Version 2.12.36.
- - - - - - - - - - - - - - - - - - - - - - - - - - - - -
==>C:\Progra~2\Presence\presence.exe
==>i=hahoba_7_lact14.pao
==>l=pres_psi_th0()_th1()_gam()_eps()_p(Season)_th0pi(PopSqMiClass).out
==>name=psi,th0(),th1(),gam(),eps(),p(Season),th0pi(PopSqMiClass)
==>j=hahoba_7_lact14.dm
seed=-1579118425
varcov: nsig=6 eps=1.000000e-002
no model name N,T-->85,144


********* Input Data summary *******
Number of sites               = 85
Number of sampling occasions   = 144
Number of states              = 2
Number of missing observations = 0
NSiteCovs-->7
site_covname[0]="siteID"
site_covname[1]="ElevMn"
site_covname[2]="PctTrees"
site_covname[3]="PopSqMi"
site_covname[4]="ElevClass"
site_covname[5]="PctTreesClass"
site_covname[6]="PopSqMiClass"
NSampCovs-->2
samp_covname[0]=Model
samp_covname[1]=Month
Primary periods=9 Secondary periods: 16 16 16 16 16 16 16 16 16
- - - - - - - - - - - - - - - - - - - - - - - - - - - - -
 file=c:\hahoba_2019_presencefiles\y.pao
- - - - - - - - - - - - - - - - - - - - - - - - - - - - -
N=85 T=144 Groups=1 bootstraps=0

-->9-16

Multi-season-Correlated-Detections model -
=============================================

9 Primary periods
  Secondary periods: 16 16 16 16 16 16 16 16 16

Model(1):psi,th0(),th1(),gam(),eps(),p(Season),th0pi(PopSqMiClass)

Open Population Model:

Model has been fit using the logistic link.


Number of parameters           = 11
Number of function calls           = 616
-2log(likelihood)              = 2098.2423
AIC                            = 2120.2423
CPU time to compute varcov matrix: 0.0 min.
```

```
Untransformed Estimates of coefficients for covariates (Beta's)
======================================================================
                                           estimate    std.error
A1   psi.a1                         :  -0.214983    0.384849
A2   th0[9-16].a2                   :  -2.711298    0.243383
A3   th1[9-16].a3                   :   1.544664    0.244483
B1   gam(8).b1                      :  -2.767336    0.426924
C1   eps(8).c1                      :  -2.444308    0.524790
D1   P[9-16].d1                     :   0.139175    0.319486
D2   P[6-16].d2                     :  -0.414862    0.202352
D3   P[7-16].d3                     :  -1.098396    0.258398
D4   P[8-16].d4                     :  -0.321290    0.268766
E1   th0pi(9).e1                    :   0.422792    0.534062
E2   th0pi(1)."PopSqMiClass"        :  -1.771050    0.585476

   Individual Site estimates of <psi>
                Site                estimate  Std.err   95% conf. interval
psi             1 1               :  0.4465   0.0951     0.2750 -  0.6317

   Individual Site estimates of <th0[1-1]>
                Site                estimate  Std.err   95% conf. interval
th0[1-1]        1 1               :  0.0623   0.0142     0.0396 -  0.0967

   Individual Site estimates of <th1[1-1]>
                Site                estimate  Std.err   95% conf. interval
th1[1-1]        1 1               :  0.8241   0.0354     0.7437 -  0.8833

   Individual Site estimates of <gam(1)>
                Site                estimate  Std.err   95% conf. interval
gam(1)          1 1               :  0.0591   0.0237     0.0265 -  0.1267

   Individual Site estimates of <eps(1)>
                Site                estimate  Std.err   95% conf. interval
eps(1)          1 1               :  0.0799   0.0386     0.0301 -  0.1953

   Individual Site estimates of <P[1-1]>
                Site                estimate  Std.err   95% conf. interval
P[1-1]          1 1               :  0.5347   0.0795     0.3806 -  0.6825
P[2-1]          1 1               :  0.3977   0.0485     0.3076 -  0.4954
P[3-1]          1 1               :  0.2500   0.0485     0.1673 -  0.3562
P[4-1]          1 1               :  0.4204   0.0655     0.2998 -  0.5512
P[5-1]          1 1               :  0.5347   0.0795     0.3806 -  0.6825
P[6-1]          1 1               :  0.3977   0.0485     0.3076 -  0.4954
P[7-1]          1 1               :  0.2500   0.0485     0.1673 -  0.3562
P[8-1]          1 1               :  0.4204   0.0655     0.2998 -  0.5512
P[9-1]          1 1               :  0.5347   0.0795     0.3806 -  0.6825

   Individual Site estimates of <th0pi(1)>
                Site                estimate  Std.err   95% conf. interval
th0pi(1)        1 1               :  0.6042   0.1277     0.3489 -  0.8130
th0pi(1)        2 2               :  0.2062   0.0665     0.1048 -  0.3654


 DERIVED parameters
      th0(1) = th0pi*th0 + (1-th0pi)*th1 = Pr(1st segment is used)

        Site                      th0(1)  Std.err     95% conf. interval
th0(1)          1 1               :  0.5226   0.1017     0.3232 - 0.7220
th0(1)          2 2               :  0.2194   0.0516     0.1182 - 0.3205
```

DERIVED parameters - psi2,psi3,psi4,...

	Site			psi(t)	Std.err	95% conf. interval
psi(2)	1	1	:	0.4435	0.0798	0.2872 - 0.5999
psi(3)	1	1	:	0.4410	0.0693	0.3051 - 0.5769
psi(4)	1	1	:	0.4388	0.0635	0.3145 - 0.5632
psi(5)	1	1	:	0.4370	0.0614	0.3167 - 0.5573
psi(6)	1	1	:	0.4354	0.0620	0.3138 - 0.5570
psi(7)	1	1	:	0.4340	0.0644	0.3078 - 0.5601
psi(8)	1	1	:	0.4328	0.0676	0.3004 - 0.5652
psi(9)	1	1	:	0.4317	0.0710	0.2925 - 0.5710

DERIVED parameters - lam2,lam3,lam4,...

	Site			lam(t)	Std.err	95% conf. interval
lam(2)	1	1	:	0.9934	0.0479	0.8995 - 1.0874
lam(3)	1	1	:	0.9943	0.0418	0.9124 - 1.0762
lam(4)	1	1	:	0.9951	0.0364	0.9238 - 1.0664
lam(5)	1	1	:	0.9957	0.0316	0.9338 - 1.0577
lam(6)	1	1	:	0.9963	0.0274	0.9425 - 1.0501
lam(7)	1	1	:	0.9968	0.0238	0.9502 - 1.0435
lam(8)	1	1	:	0.9972	0.0206	0.9568 - 1.0377
lam(9)	1	1	:	0.9976	0.0178	0.9627 - 1.0326

CPU time= 8 seconds (0.13 min)

PRESENCE - Presence/Absence-Site Occupancy data analysis
Wed Jan 15 12:00:25 2020,   Version 2.12.36.
- -